Asymptotic Effect of Initial and Upstream Conditions on Turbulence

William K. George
Marie Curie Intra European Principal Research Fellow
Department of Aeronautics,
Imperial College of Science, Technology and Medicine,
South Kensington Campus,
Exhibition Road, SW7 2AV, London, UK
e-mail: georgewilliamk@gmail.com

*More than two decades ago the first strong experimental results appeared suggesting that turbulent flows might not be asymptotically independent of their initial (or upstream) conditions (Wygnanski et al., 1986, "On the Large-Scale Structures in Two-Dimensional Smalldeficit, Turbulent Wakes," J. Fluid Mech., **168**, pp. 31–71). And shortly thereafter the first theoretical explanations were offered as to why we came to believe something about turbulence that might not be true (George, 1989, "The Self-Preservation of Turbulent Flows and its Relation to Initial Conditions and Coherent Structures," Advances in Turbulence, W. George and R. Arndt, eds., Hemisphere, New York, pp. 1–41). These were contrary to popular belief. It was recognized immediately that if turbulence was indeed asymptotically independent of its initial conditions, it meant that there could be no universal single point model for turbulence (George, 1989, "The Self-Preservation of Turbulent Flows and its Relation to Initial Conditions and Coherent Structures," Advances in Turbulence, W. George and R. Arndt, eds., Hemisphere, New York, pp. 1–41; Taulbee, 1989, "Reynolds Stress Models Applied to Turbulent Jets," Advances in Turbulence, W. George and R. Arndt, eds., Hemisphere, New York, pp. 29–73) certainly consistent with experience, but even so not easy to accept for the turbulence community. Even now the ideas of asymptotic independence still dominate most texts and teaching of turbulence. This paper reviews the substantial additional evidence - experimental, numerical and theoretical - for the asymptotic effect of initial and upstream conditions that has accumulated over the past 25 years. Also reviewed is evidence that the Kolmogorov theory for small scale turbulence is not as general as previously believed. Emphasis has been placed on the canonical turbulent flows (especially wakes, jets, and homogeneous decaying turbulence), which have been the traditional building blocks for our understanding. Some of the important outstanding issues are discussed; and implications for the future of turbulence modeling and research, especially LES and turbulence control, are also considered.* [DOI: 10.1115/1.4006561]

Foreword

Over the past two decades, a quiet paradigm shift has been taking place in our understanding of turbulent flows. It appears, contrary to long-held beliefs, that the space-time development of turbulence can be influenced, even asymptotically, by its initial and/or upstream conditions. Although documented by an increasing number of researchers and in the most reputable journals, this understanding has for the most part not made its way into most of the recent texts on turbulence. As a result, engineers (and most fluid dynamicists for that matter) fall into two camps: those few who have stumbled onto the new way of thinking through their research, and the great majority who have continued to be trained in the old way of thinking. Unfortunately, this division considerably complicates communication at almost every level, from the review of manuscripts for publication and proposals for funding, to even understanding why certain lines of research should be pursued at all. It also affects the attitude toward turbulence research in general, with those educated in the new school finding the field vibrant and exciting, while the others tending think of it as old and stagnant and lacking new ideas. Even one of the most important research applications at the moment, turbulence control, finds itself caught between two worlds: one world in which control is demonstrated in at least some circumstances to be possible, and a second world in which turbulence is believed to be asymptotically independent of initial conditions, *and therefore by definition uncontrollable*. But even those who claim to religiously believe in asymptotic independence and teach it in their classrooms often still accept the money from their sponsors to seek to control turbulence. This confuses both student and sponsor alike, and makes the field appear to be incoherent – which in fact it is! As a result, opportunities are lost, new entrants become discouraged and give up, and the field wobbles forward more like a religion or political philosophy whose basic tenets have been proven wrong, than a vibrant scientific discipline seeking to increase knowledge and improve application.

This review paper on turbulent shear flows will attempt to show how the turbulence community came to believe the traditional views, why those ideas were almost right, and what was wrong with them. Then it will show how the breakthroughs of two and one-half decades ago changed things, and continue to do so. Finally it will try to provide an honest assessment of our understanding today, and to identify what we would still like to know and how we might find it. In the absence of firm theoretical foundations, there would seem to be little point in discussing the many implications for applications, so I shall for the most part leave those discussions to those who follow me. Therefore (and upon the advice of a former Freeman scholar) I shall deliberately restrict the scope of this survey, and focus only on the question of whether initial and upstream conditions affect turbulence asymptotically, and what this might imply about our understanding of turbulence.

Contributed by the Fluids Engineering Division of ASME for publication in the JOURNAL OF FLUIDS ENGINEERING. Manuscript received March 11, 2012; final manuscript received March 14, 2012; published online June 11, 2012. Assoc. Editor: Malcolm J. Andrews. Proceedings of the ASME 2008 Fluids Engineering Meeting, 2008 Freeman Lecture, August 10-14, 2008, Jacksonville, FL, USA, FEDSM2008-55362.

Historical Background

The question of whether initial conditions (in time-developing flows) or upstream conditions (in spatially-developing flows)

affect turbulence has been of interest for a long time, and in fact was even the subject of an earlier Freeman lecture by Hussain [1]. In spite of persistent and annoying discrepancies from one experiment to another (e.g., the seeming endless debate about the spreading rates of jets), almost all of the attention was focused on turbulence in the early stages of development. There was little serious debate until almost a decade later about whether these effects persisted asymptotically. And even today, textbooks routinely ignore the possibility that free shear flows and homogeneous flows might be asymptotically different.

The Pandora's box was opened by Bevilaqua and Lykoudis [2] who showed very different asymptotic behavior for two different wake generators, but their results were not widely accepted (e.g., Sreenivasan and Narasimha [3]). It was a publication in 1986 of the careful plane wake experiments of Wygnanski, Champagne, and Marasli [4] that pretty much shook the foundations of traditional thinking about turbulence. For more than 50 years the traditional view (v. almost any book on turbulence, e.g., [5,6]) of turbulence had been that the wake far downstream from the generator should depend only on the drag on the wake generator and the downstream distance from it (measured from some virtual origin). By substituting screens with the same drag but with differing solidity for an airfoil or strip, they were able to maintain a constant drag (and hence fix the crucial scaling parameters). As expected, the mean velocity profiles beyond an adjustment region collapsed from one generator to another using only the centerline velocity deficit and a local measure of the wake thickness as shown in Fig. 1. In fact it was mean velocity measurements like this in the first place that had led to acceptance of the view that such free shear flows were asymptotically independent of upstream conditions. Contrary to all expectations (see any book on turbulence, even the new ones), they found that the same collapse could not be achieved for the spreading rate, the turbulence intensities, nor the Reynolds shear stress (see Figs. 2, 3, 4 and 5). The turbulence intensities and Reynolds shear stress profiles could only collapsed for a particular wake generator, and not with each other. Moreover, the different spreading rates varied by as much as *several hundred percent*!

They summarized their findings as follows:

> "Sreenivasan and Narasimha [3]) suggested that a unique self-preserving state exists for all plane wakes and defined the characteristic constants stemming from their suggestion. We felt at the time that their data did not fully support their conclusion, and the present study compiles further evidence negating it…. It was experimentally observed (by the authors *sic*) that the characteristic velocity and length scales…, when suitably scaled by the momentum thickness and the free-stream velocity, do not exhibit universal behavior and do depend on the inflow conditions and therefore on the geometry of the wake generator. The mean velocity profiles for each wake, when normalized by their own velocity and length scales, are self-preserving and are also identical for all wake generators. The distributions of the turbulence intensities normalized in the same manner are almost self-preserving, but they are dependent on the geometry of the wake generator."

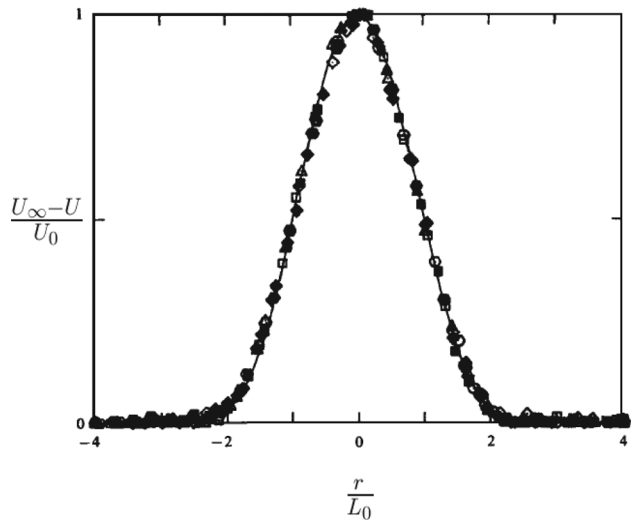

Fig. 1 Asymptotic normalized mean velocity profiles of four different plane wake generators (strip, airfoil and two screens of different solidity, all with same drag) (from Wygnanski et al. [4]). Mean velocity normalized with centerline deficit velocity and lateral coordinate with momentum thickness.

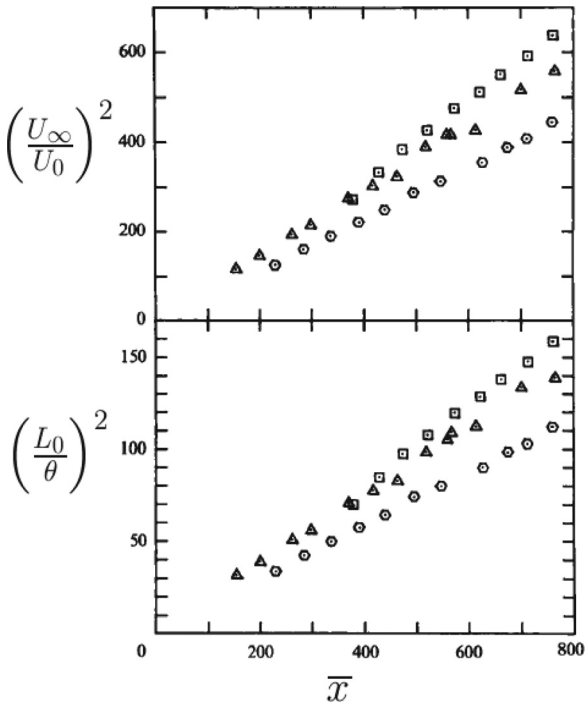

Fig. 2 Plane wake plots showing how spreading rate and centerline velocity decay rate depend on wake generator (squares: airfoil; triangles: 70% solidity screen; hexagons: solid strip) and normalized downstream distance from a virtual origin $\overline{x} = (x - x_o)/2\theta$, from Wygnanski et al. [4]

These new results unequivocally called into question almost a half century of how we think about and model turbulence. Unless proven wrong, they clearly invalidated the traditional thinking, which presumes the asymptotic wake from *any* wake generator as

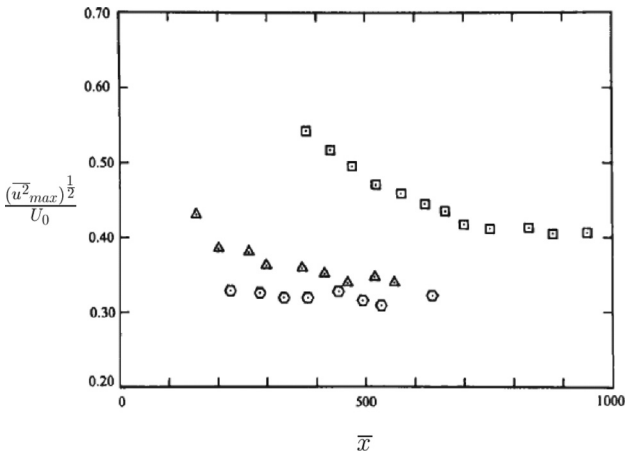

Fig. 3 Downstream variation of centerline plane wake turbulence intensities showing asymptotic dependence on wake generator (squares: airfoil; triangles: 70% solidity screen; hexagons: solid strip) and normalized downstream distance from a virtual origin, $\overline{x} = (x - x_o)/2\theta$, from Wygnanski et al. [4]

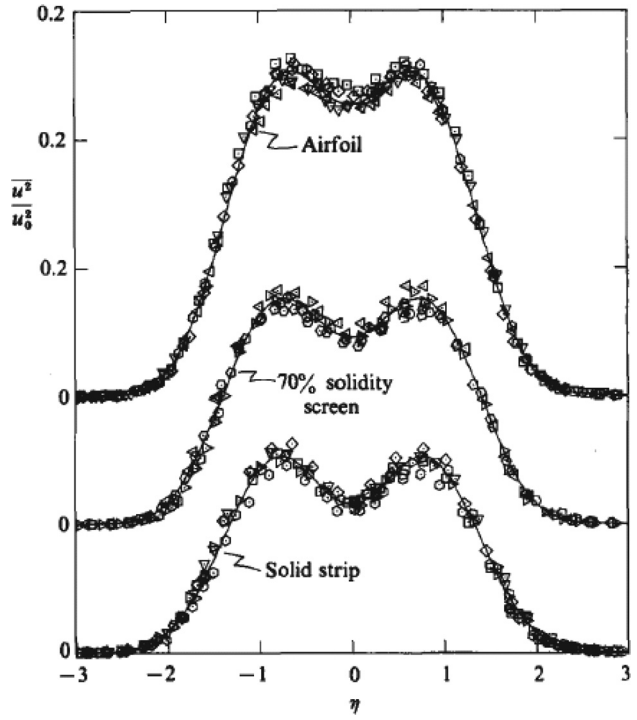

Fig. 4 Plane wake turbulence intensity profiles normalized by centerline velocity deficit showing dependence on wake generator and normalized downstream distance from a virtual origin $\overline{x} = (x - x_o(/2\theta)$, from Wygnanski et al. [4]

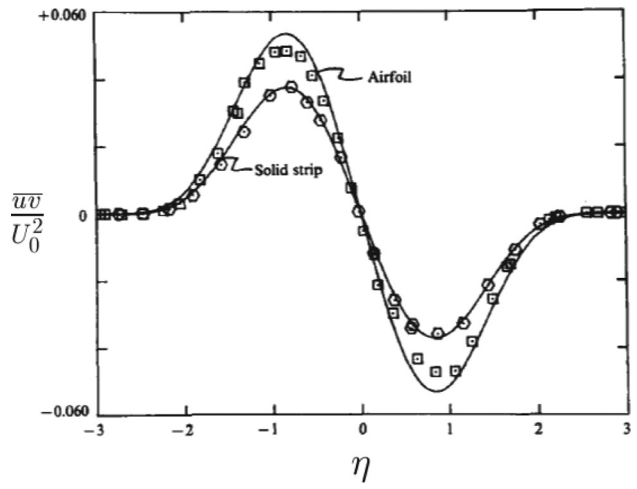

Fig. 5 Reynolds shear stress normalized by centerline velocity deficit for cylinder and screen showing dependence on wake generator, from Wygnanski et al. [4]

developing from a point sink of momentum, and thus depending only on the drag of the generator.

My first introduction to these revolutionary ideas and findings was a private discussion with Frank Champagne (Professor, University of Arizona) at the Turbulent Shear Flow conference at Cornell a few years before publication. Like most of the turbulence community I believed their results could not possibly be correct; and that they had either done something wrong, or had not simply gone far enough downstream. This argument is still used by some today in spite of all evidence to the contrary. My concerns about whether the data satisfied the differential equations and the homogeneous boundary conditions were met with assurance that they did. The work was ultimately published, not because the reviewers were particularly happy about the results,

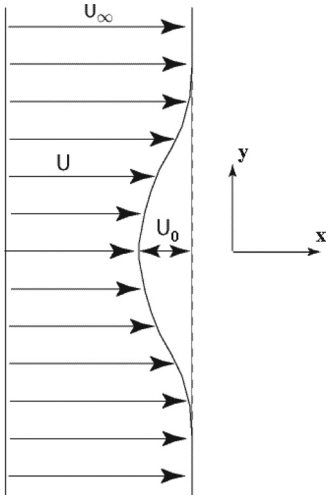

Fig. 6 Schematic of far wake showing coordinates and symbols

but because of the reputation of the investigators and the evident (and indisputable) care taken in the measurements.

Almost concurrent with publication was the second important breakthrough, this time theoretical and my own. In the fall of 1986, I was teaching a class on turbulence at the State University of New York at Buffalo. A Ph.D. student in the course (Jin-Ho Lee) asked about why it was reasonable to assume the Reynolds shear stress to be scaled in a shear flow by the same velocity scale as the mean velocity profile. Working without my notes, I answered him by hypothesizing the scales to be different, confident that I could prove them to be the same. Since the arguments are both easy to understand and quite crucial to all that follows, I will repeat them here.

A schematic of the flow under consideration is shown in Fig. 6. In their simplest form, the Reynolds-averaged streamwise momentum equation for a far plane wake in a uniform and constant mean stream can be shown to reduce to [7]

$$\frac{\partial}{\partial x}(U - U_\infty) = \frac{\partial}{\partial y}\langle -uv \rangle \tag{1}$$

where U_∞ is the free stream velocity. The boundary conditions are assumed homogeneous except for on the surface of the wake generator.

Since no forces are assumed to act downstream from the wake generator, the flow is characterized by a constant kinematic momentum deficit, i.e.,

$$D_o = U_\infty^2 \theta = \int_{-\infty}^{\infty} U(U_\infty - U)dy \approx U_\infty \int_{-\infty}^{\infty} (U_\infty - U)dy \tag{2}$$

where ρD_o is the drag per unit length on the wake generator and the approximation improves with increasing distance downstream as the wake spreads and the centerline velocity deficit, $U_o = U_\infty - U_{cl}$, weakens.

Without loss of generality we seek similarity solutions of the form

$$U - U_\infty = U_s(x) f(\eta, *) \tag{3}$$

$$-\langle uv \rangle \quad = R_s(x) g(\eta, *) \tag{4}$$

where $\eta = y/\delta$. $\delta = \delta(x)$, $U_s = U_s(x)$ and $R_s = R_s(x)$ are unspecified scaling functions which vary downstream, but must be determined from the solution and boundary conditions. The mean

velocity dimensionless profile function, $f(\eta,*)$ and the dimensionless Reynolds shear stress function, $g(\eta,*)$ are both functions of the scaled transverse coordinate, η. The argument, $*$, represents any possible dependence on upstream conditions, and must in principle be retained unless the profile functions can be shown to be independent of them.

Applying the chain-rule for differentiation and substituting into Eq. (1) yields the following equation

$$-\left[\frac{U_\infty U_s}{\delta}\frac{d\delta}{dx}\right](\eta f)' = \left[\frac{R_s}{\delta}\right]g' \tag{5}$$

where $'$ denotes differentiation with respect to η. Note that all of the explicit x-dependence is the square-bracketed terms. Also note that to this point, the equations have simply been transformed into different independent variables, and no assumptions have been made (beyond those made in writing the original equations).

The whole idea of a similarity solution (of any kind) is that the profiles themselves become independent of the downstream coordinate. This can happen only *if the flow has achieved an equilibrium in which the terms in governing equations maintain the same relative balance as it continues to develop in the downstream direction*. So now we choose to seek solutions which satisfy exactly this condition, the so-called '*equilibrium similarity assumption*.' We need not worry about whether such solutions are possible, since if the equations do not admit to such solutions, none will be found. Nontrivial solutions of Eq. (4) can be x-independent only if the x-dependence of the equation itself vanishes. Clearly this is possible only if

$$\left[\frac{U_\infty U_s}{\delta}\frac{d\delta}{dx}\right] \propto \left[\frac{R_s}{\delta}\right] \tag{6}$$

or by simply defining

$$R_s = U_s U_\infty \frac{d\delta}{dx} \tag{7}$$

In words: the scale for the Reynolds stress scaling functions, R_s must be proportional to the spreading-rate, $d\delta/dx$, of the wake itself!

The classical theory not only assumes independence of upstream conditions, it also assumes that $R_s = U_s^2$ (see, for example, Tennekes and Lumley [6], Townsend [5]). I could not then, nor can I till this day, make $R_s = U_s^2$, at least *without assuming them to be the same or by making an equivalent assumption somewhere else*. In fact to my surprise, it was not even necessary for R_s and U_s^2 to be the same, since a similarity solution can clearly be achieved without it. And even if they are proportional (as in the infinite Reynolds number solution), *the coefficient need not be universal, but could depend on the initial conditions* [7]. More surprising, once one relaxed the over-constraint of the classical single-length, single-velocity scale hypothesis, several new features came to light: even though the normalized mean velocity profiles could be shown to collapse independent of upstream conditions, the spreading rates (see Fig. 1) were in principle dependent on them, as were the higher turbulence moment profiles (including Reynolds shear stress). It was recognized almost immediately that this had important implications for turbulence modeling, and had the consequence that no universal single point model was possible, since the initial conditions would appear in the model coefficients [7,8].

This methodology applied to several other example flows was first presented at an invited session of the American Society of Civil Engineers meeting in Minneapolis in 1986[1], and subsequently appeared in contributions [7,8] to the volume that came out of it [9]. Over the next few years, my co-workers and I were able to apply some of the same general *equilibrium similarity*[2] ideas to several homogeneous flows, including with temperature fluctuations (George [11], [12]) and mean shear (George and Gibson [13]). The conclusions were the same—asymptotic dependence on initial conditions—and generally in agreement with the available experiments (e.g., Comte-Bellot and Corrsin [14,15], Wahrhaft and Lumley [16], Rohr et al. [17], Gibson and Kanellopoulos [18] and others). And even later, Luciano Castillo and I were able to show theoretically the possibility that the outer (or main) part of turbulent boundary layers could behave the same way (v. George and Castillo [19], Castillo and George [20]).

The response of the field throughout the 1980s and most of the 1990s to the experiments, theory and their implications was largely disbelief, and at best benign disinterest. This situation persisted in spite of publication of the axisymmetric wake experiments of Cannon et al. [21], further plane wake studies by Zhou and Antonia [22,23], and the DNS studies of Boersma et al. [24] on turbulent jets. But led by Antonia and his co-workers at the University of Newcastle in Australia, other investigators began to notice (or at least report) the same effects in their own work. Since 2000, there has been an ever increasing parade of experimental and computational results, most finding some asymptotic dependence on initial conditions. Sometimes the effects can be dramatic, sometimes less so. Oftentimes, the studies were carefully performed and the right questions asked; however, sometimes this was not the case. In the following sections I shall try to summarize some of these developments, and try to indicate how future studies might be more definitive. Over the past 20 years, there have been literally thousands of papers which have been published about initial conditions in turbulence. I have restricted attention to those classes of flows for which equilibrium similarity solutions have been found, since these most clearly allow distinguishing the roles of initial (and/or upstream) conditions from other external conditions (e.g., boundary conditions, facility effects, etc.).

Free Shear Flows

Observations in free shear flows have been in the forefront of those studies of flows for which equilibrium similarity solutions exist, none more so than the plane wake which began this field of inquiry. Other free shear flows that have received considerable attention, both experimentally and numerically, are the axisymmetric wake and round jet, the latter with and without net mass flow and swirl. Each of these will be considered below. The zero-net-mass flow jet and swirling jet will be seen to be of considerable importance, since they highlight the importance of scaling things correctly before a judgment as to the effect of upstream conditions can be made.

The Plane Wake. Since publication of the Wygnanski et al. [4] paper, there have been a number of studies which have confirmed and added to them. The experimental studies of Zhou and Antonia [22,23], Rinoshika and Zhou [25] are of special interest, since the authors found essentially the same results in different facilities. Like the earlier experiments, they found the mean velocity profiles to collapse when normalized by the local centerline velocity deficit and the local length scale. Also like the earlier study they found the Reynolds stress profiles to collapse only for a given upstream wake generator. Of particular interest was the following observation:

> "The difference is especially noticeable between the wake of the screen and the solid-body wakes. For the screen, the far-field vortices are highly similar to the near-field ones. For the solid-body wakes, the far-field vortices bear little resemblance to the near-field vortices]" [23].

[1]The session was put together to honor one of my early mentors, Prof. Stanley Corrsin of the Johns Hopkins University, upon the occasion of his being awarded the von Kármán medal. Sadly he died a few days before. This work was the subject of my discussion with him during a visit a few months before his death.

[2]Note that it was not until 1995 [10] that I introduced the term '*equilibrium similarity*' to distinguish the methodology from 'self-preservation' which seemed to many people to imply the single-length/single velocity scale hypothesis.

All of these were consistent with the theoretical arguments from equilibrium similarity, including the suggestion of Wygnanski et al. [4] and George [7] that it was the large scale motions that were responsible for the differences.

The equilibrium similarity arguments also received substantial support from the DNS results of Moser et al. [26] for the unsteady (or time-dependent) plane wake. In this case, the flow was homogeneous in the streamwise and spanwise directions, inhomogeneous across the wake, and nonstationary in time. Several cases were computed, one unforced, the other two differently forced at the lowest wavenumber. These time-dependent wakes grew as expected from the equilibrium similarity theory at different rates until they began to exhibit strong roller eddies, indicating the influence of the finite boundaries. Because of this, departures from the theory were particularly useful for identifying when the flow computations began to be influenced by the finite computational region. A second and more recent paper by Ewing et al. [27] using the same data showed that that even the two-point statistics behaved as described by equilibrium similarity. Figures 7 and 9 show the unscaled (raw) spectral data in physical variables, while Figs. 8 and 10 show the same data in similarity variables. The authors described their spectral results as follows:

> "There appear to be short ranges of $k^{-5/3}$-range in the spectra from both wakes. These ranges are of greater extent in the forced wake because the turbulence Reynolds number of these flow is greater. The spectra from the forced wake also have a larger energy content in the low wavenumber region because of the organized structures present in this wake owing to the initial forcing. The spectra in both wakes decrease in magnitude and shift to lower wavenumbers as the wakes evolve, as predicted in the analysis."

Rogers [28] took the same unsteady time-dependent wake data and subjected it to ten different straining motions. *All of the results were consistent with equilibrium similarity solutions, suggesting strongly that if such solutions can be found, they can be realized.* This is, of course, contrary to the conventional wisdom of the day. Interestingly, Rogers found some of the solutions by postulating an equilibrium between different groups of terms, groupings consistent with their order of magnitude and importance.

Finally, and perhaps most interesting of all from the perspective of this paper, was the time-dependent plane wake LES by Ghosal and Rogers [29]. By forcing the largest scales they were able to achieve a variety of growth rates, all consistent with the equilibrium similarity solutions, at least until the computation was affected by the finite size of the computational domain. In particular, all the mean velocity profiles collapsed together, the Reynolds normal stresses were distinct for each set of initial conditions, but

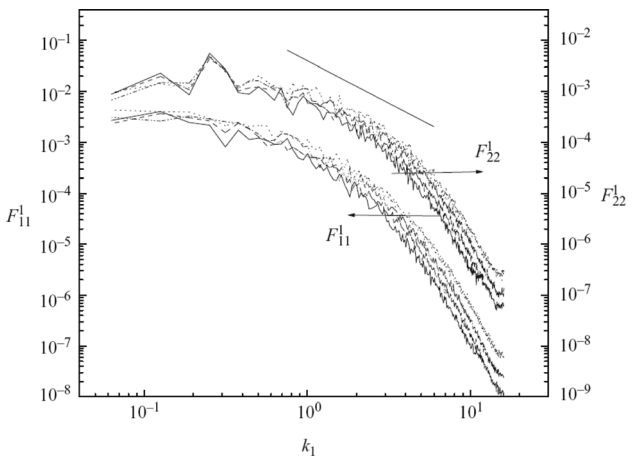

Fig. 7 Streamwise velocity spectra from unforced wake at centerline for four different times during wake decay, from Ewing et al. [27]

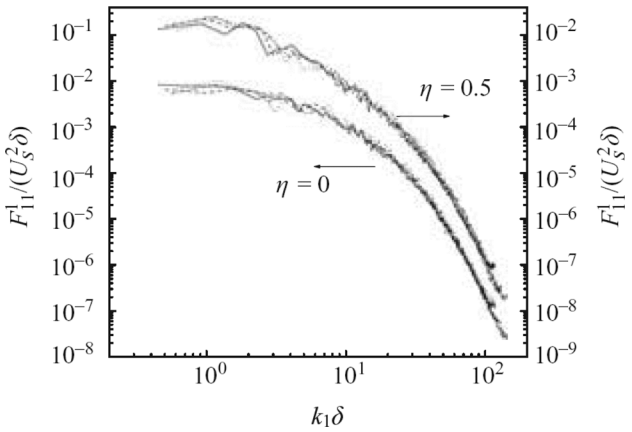

Fig. 8 Normalized streamwise velocity spectra from unforced wake at centerline and $\eta = r/\delta_{1/2} = 0.5$, from Ewing et al. [27]

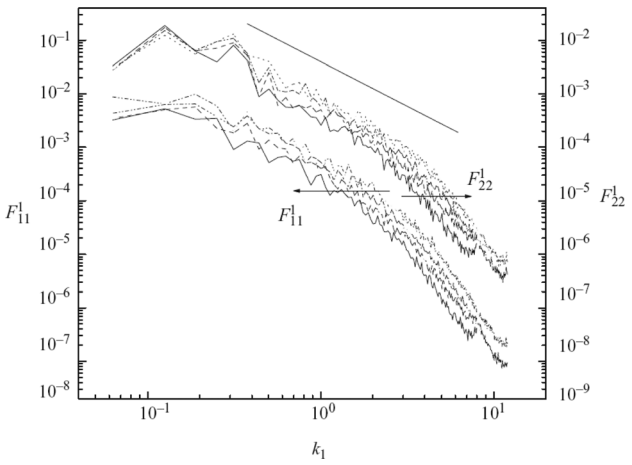

Fig. 9 Streamwise velocity spectra from forced wake at centerline for four different times during wake decay, from Ewing et al. [27]

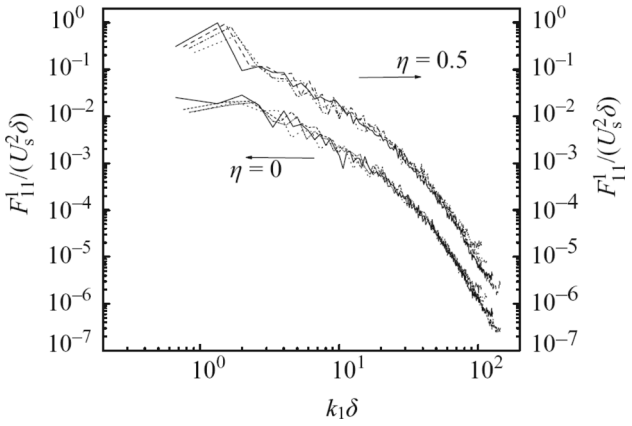

Fig. 10 Normalized streamwise velocity spectra from forced wake at centerline and $\eta = r/\delta_{1/2} = 0.5$, from Ewing et al. [27]

the Reynolds shear stress could be collapsed for all cases by using the growth-rate (as demanded by the theory). This result could be viewed as a ray of hope in an otherwise '*inconvenient truth*'[3], since it makes it clear that however the turbulence retains

[3]Acknowledgment to Al Gore.

information on its origins, it is apparently preserved through the LES closure approximations.

The Axisymmetric Wake. In 1987 at the American Physical Society meeting in Eugene, OR, I showed my equilibrium similarity analysis of the plane wake to Israel Wygnanski for the first time, and showed him how it could account for their plane wake observations. Intrigued, he immediately challenged me to predict the behavior of the axisymmetric wake experiments that they had already begun at the University of Arizona. I spent a good bit of the night pondering the matter and returned the next day with my response: 'I think you will see the same strong dependence on the wake generator, but I really am not sure how rapidly the wake will decay. There seem to be two solutions: one which decays as $x^{1/2}$, and the other classical solution [6] which decays as $x^{1/3}$. And I am not sure which solution one might observe in the laboratory, nor whether one could evolve into the other' (note that the $x^{1/2}$ solution was not the laminar flow solution, although it decayed the same way, but a fully turbulent low Reynolds number solution). I was informed that the first part about the initial conditions was correct, and that the issue of how the wake decayed was exactly the dilemma presented by the measurements themselves. So in George [7] I discussed both possibilities. It was not until many years later, hindsight being 20:20, that the answer became obvious.

The University of Arizona axisymmetric wake experiments, subsequently reported by Cannon and Champagne [21,30], showed quite convincingly the expected behavior (see Figs. 11 and 12); namely, that the upstream conditions affected significantly both the spreading rates and the nature of the coherent structures. Like the plane wake and as expected from the theory, the mean velocity profiles also collapsed from all experiments. Figures 13 and 14 show the mean velocity profiles from the disk experiments of Cannon [30] and as well that of Ref. [32]. But the Arizona data was inconclusive for choosing between the two alternatives for the decay of the centerline velocity deficit and the spreading rate. It was not until a decade later that the experiments of Johansson et al. [31] and Johansson and George [32] that it became clear exactly what was happening. In fact, unlike the plane wake and axisymmetric jet

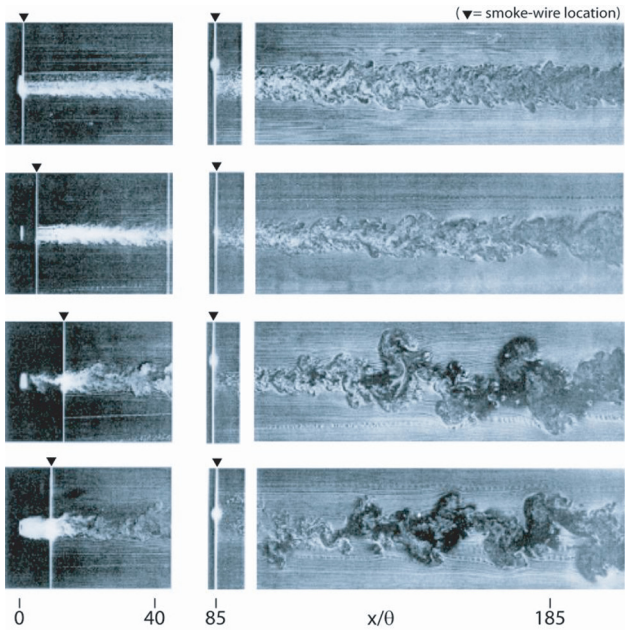

Fig. 11 Far wakes from four different wake turbulence generators from Cannon et al. [21] showing strong dependence of large scale features on generator even far downstream. From top: screens of solidity 0.50, 0.60, 0.85 and solid disk, all at Reynolds number based on free stream velocity and momentum thickness of approximately 3500.

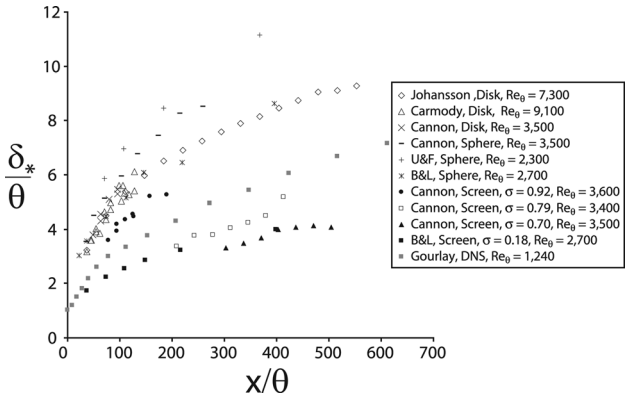

Fig. 12 Cross-stream length scale, δ_*/θ versus x/θ. For the screen wakes, the porosity is defined as σ = (solid area)/(total area). From Johansson et al. [31].

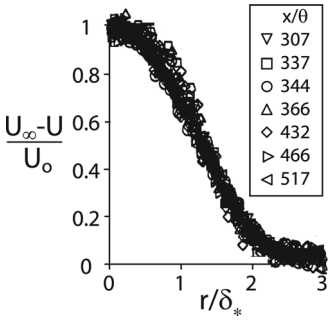

Fig. 13 Mean velocity deficit profiles, disk data from Cannon [30]

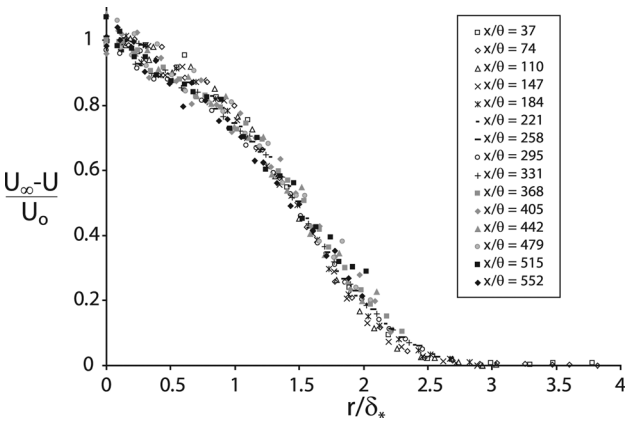

Fig. 14 Mean velocity profiles, disk data from Johansson and George [32]

flows, the local Reynolds number for the wake, say, $U_o\delta/\nu$, is not constant, but drops slowly. So no matter how high the Reynolds number at the axisymmetric wake generator, nor how unimportant the viscous terms actually are in either the equations for the mean flow or turbulence near the generator, they eventually grow back into both as the wake decays, especially the latter. At very high initial Reynolds number, the wake centerline velocity deficit decays as $U_o \propto x^{-2/3}$ and the wake width grows as $\delta \propto x^{1/3}$, exactly like the classical solution except for the dependence of the coefficients on the wake generator. But contrary to the earlier view that the wake simply laminarizes, it falls into a second equilibrium similarity state, a low-Reynolds number turbulent state if you will, in which the centerline velocity deficit decays as $U_o \propto x^{-1}$ and the

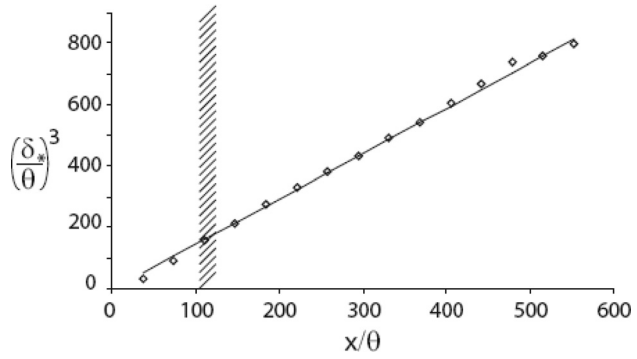

Fig. 15 Spreading rate for the high Reynolds number axisymmetric disk wake of Johansson and George [32]. Cross-hatched region shows approximate lower limit of validity of infinite Reynolds number solution.

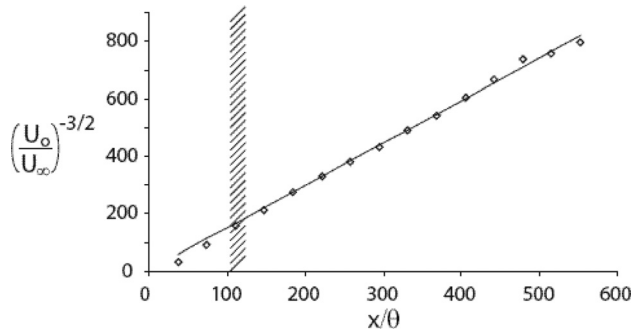

Fig. 16 Centerline velocity deficit decay rate for the high Reynolds number axisymmetric disk wake of Johansson and George [32]

wake spreads as $x^{1/2}$. In this state the viscous stresses and viscous transport terms in the Reynolds stress equations remain as important as the Reynolds stress production, which keeps producing turbulence energy by working against the mean flow gradient. So even though the wake gets weaker and weaker, its dynamics are still fully turbulent. Since one can never really have an infinite Reynolds number in an experiment or simulation, nor are wind tunnels long enough to reach the viscous-dominated state, the typical experiment finds itself between these extremes: hence the dilemma of Cannon [30] in establishing exactly what the power law dependence was from experimental data alone.

In fact the second solution has only been truly observed in the very long time time-dependent-wake DNS of Gourlay et al. [33] (see also Johansson et al. [31]). Figures 15 and 16 illustrate the high Reynolds number solution using experimental data from behind a disk by Johansson and George [32]. These data are characterized by a $k^{-5/3}$ range in the velocity spectra, indicating clearly the high Reynolds number nature of the solution which is based on the idea that the dissipation can be approximated as $\varepsilon \propto u^3/\delta$. The high Reynolds number solution also appears initially in the DNS data of Gourlay et al. [33], but it eventually evolves to the low Reynolds number solution shown in Figs. 17 and 18. Note the extremely large values of x/θ at which the low Reynolds number appears. For this region there is no $k^{-5/3}$ range in the velocity spectra, consistent with the low Reynolds number approximation used for the dissipation, $\varepsilon \propto \nu u^2/\delta^2$.

Jets

Overview. Jets, like those shown in Fig. 19, are often created by flow exhausting from nozzles. Typically they go through an adjustment region that can be from a few to many diameters (for high Mach number and/or low Reynolds number flows) before they reach an asymptotic state. The most interesting cases theoretically, at least from the perspective of this article, are those exhausting into a quiescent environment. This is because these are

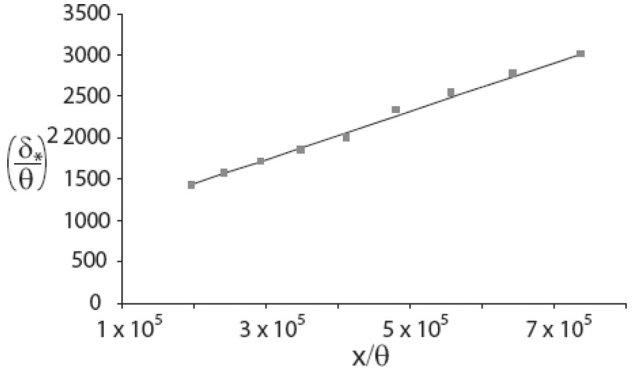

Fig. 17 Spreading rate for low Reynolds number axisymmetric wake from DNS of Gourlay et al. [33]. Note the extremely large values of x/θ at which the low Reynolds number solution is observed, from Johansson et al. [31].

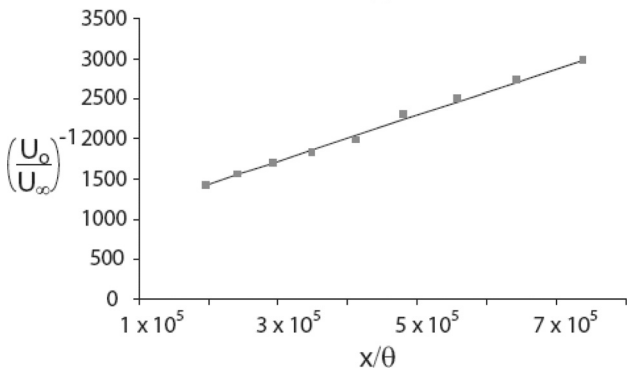

Fig. 18 Centerline velocity deficit for low Reynolds number axisymmetric wake from DNS of Gourlay et al. [33]. Note the extremely large values of x/θ at which the low Reynolds number solution is observed, from Johansson et al. [31].

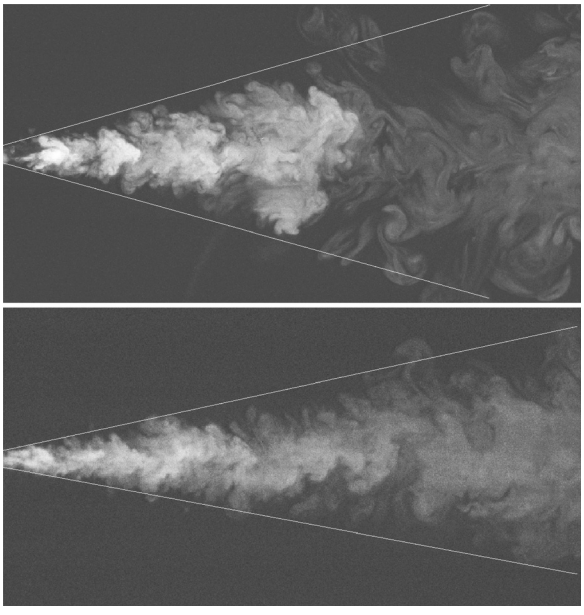

Fig. 19 Florescent dye visualizations of zero-net-mass-flux jet (above) and steady jet (below) showing 30% difference in asymptotic spreading rates, from Cater and Soria [36]

the only external conditions for which equilibrium similarity solutions (or even the classical self-preserving solutions) are possible. And in fact, this was one of the flows considered theoretically in my original article [7]. For the high Reynolds number top-hat exit profile jet (uniform flow across the exit plane) at low Mach number, it usually takes about 30 exit diameters before the asymptotic state is reached (see Panchepakesan and Lumley [34] and Hussain et al. [35]), so it is these asymptotic jets that will be primarily considered here.

The theoretical conclusions from equilibrium similarity considerations quite simply were very much like the other flows considered above: the asymptotic spreading rates reflected the source conditions, mean velocity profiles from different source conditions collapsed when plotted using the centerline velocity, U_c, and any appropriate width defined from the profile itself (like the half-width, $\delta_{1/2}$); the Reynolds stress profiles from different source conditions collapsed when normalized using $U_c^2 d\delta_{1/2}/dx$, and there was no reason to expect any of the other statistical properties from different sources to collapse at all. While there was no systematic evidence available at that time to support these deductions, it was argued that the inability of the community to agree on the rate at which axisymmetric jets actually spread was proof in itself, since no two experiments have precisely the same exit conditions. These arguments were refined in the appendix of Hussain et al. [35] and extended to plane jets in George [10].

One of the most dramatic and early experimental demonstrations of the role of upstream conditions on jets was the blooming jet experiments carried out at Stanford by Parekh et al. [37]. By forcing the jet exit periodically they were able to actually make the jet bifurcate into two separate streams, each resembling a single jet. Less dramatic were a number of experiments published subsequent to 1986 arguing for the role of exit conditions on the initial spreading rates of ordinary (steady in the mean) jets, e.g., Russ and Strykowski [38]). And there have been many since, e.g., the numerical studies of Grinstein [39,40], the swirling jet studies of Gilchrist and Naughton [41] to cite but a few. But, as noted in the introduction, it was not until the DNS jet studies of Boersma et al. [24] at the Technical University of Delft that the first systematic studies of the asymptotic jet began to appear. These DNS were carried out at relatively low Reynolds number, but the authors did not hesitate to draw conclusions from them. Quoting from their paper:

> "The results obtained from the DNS with a top-hat initial velocity profile show excellent agreement with the available experimental data of Panchapakesan and Lumley [34] and Hussein et al. [35]. The comparison of the results found with the two different initial profiles was used to check the hypothesis of universal self-similarity of a jet. The results do not support universal self-similarity. However, when we use the alternative scaling proposed by George [7] in which a dependence of the similarity on the initial conditions is kept, the agreement between both simulations becomes much better. Therefore we agree with George and conclude that the difference between data obtained in various jet experiments found in the literature may not be solely due to experimental errors but may for a large part be attributed to an incorrect scaling" (Boersma et al. [24]).

Published almost simultaneously was the experimental study, also carried out at Delft, using PIV (particle image velocimetry) of a low Reynolds number jet (2000) by Fukushima et al. [42] which showed a substantially lower spreading rate than jets at higher Reynolds number (see also Ewing et al. [43]), consistent with the arguments in the appendix of Hussein et al. [35] that source Reynolds number might be important, especially if very low. Also, experimental studies at the University of Adelaide of the passive scalar field in top-hat and pipe flow jets by Mi et al. [44] showed evidence of the effects of the source conditions on the asymptotic spreading rates. These were followed by a number of experiments, all claiming to have demonstrated the effect of source conditions and testing various aspects of the George [7] theory, confirming parts, but sometimes questioning others (e.g. Xu and Antonia [45,46], Burattini and Djendidi [47], Burattini and Antonia [48]. In their conclusions Xu and Antonia [45] summarize their results quite nicely and place them in the perspective of earlier studies:

> "In the present paper, the characteristics of a jet issuing from a smooth contraction nozzle were compared with those of a jet that exits in a fully developed turbulent state from a long pipe. The measurements in the contraction jet are in good agreement with available data (Hussein et al. [35]; Panchepakesan and Lumley [34]). The decay rate of the centerline mean velocity and the growth rate of the jet half-width agree with those of Ferdman et al. [49] for the pipe jet. They found that the far-field decay rates of the pipe jets are smaller than those with an initial top-hat velocity distribution. However, they concluded that the pipe jets develop into a self-preservation state more rapidly. The present results for the mean velocity and Reynolds stresses indicate that the contraction jet develops more rapidly than the pipe jet, the former flow approaching self-preservation more rapidly than the latter. The differences are associated with differences in turbulence structure in both near and far fields of these two flows. Spectra of v indicate significant differences in the near-field structures. For $x > 3d$, the spectral peak always occurs at a lower frequency in the pipe jet than in the contraction jet. For $x \geq 3d$, the peak is nearly at the same frequency" (from Xu and Antonia [45]).

And another interesting observation comes from the paper of Burattini and Djendidi [47], which deals with the speculation as to how source conditions might have an effect far downstream:

> "An interesting discussion on the effects of the coherent structures in the context of self-similarity was reported by George [7]. He noted that the evolution of the shear layer is dominated by a sequence of instabilities, each one triggered by the preceding one. He thus argued that the final possible self-similar state is influenced by the manner in which the flow was initiated, i.e., the initial conditions. Our results appear to corroborate George's arguments. Indeed, the introduction of the grid at the jet exit interferes with the sequence of instabilities and helps the flow to settle more rapidly towards a self-similar state" (Burattini and Djendidi [47]). Clearly this is still speculation, but it at least suggests a direction toward understanding why things are the way we find them.

It must be noted, however, that the asymptotic jet is relatively insensitive to changes in the exit profile, with differences in spreading rate typically being about 10–15%. This can be contrasted with the wake experiments cited above where the differences were measured in hundreds of percent. Thus all of the effects that make the measurement of free shear flows difficult in the first place (e.g., George [50]) make it truly difficult to establish unequivocally that source conditions have made a difference for the round jet. Therefore it is particularly important that comparisons be made appropriately. For example, what exactly is the '*equivalent*' diameter of a pipe flow jet relative to that of a top-hat jet? Or what would be the '*velocity*' corresponding to the top-hat exit velocity, say U_j, if there is a velocity profile at the exit? Surely not just the velocity maximum. As shown in the next section, the answer lies in considering integral parameters instead of simply picking parameters of convenience.

Some Scaling Issues: Mass, Buoyancy and Swirl. This question of finite sources was addressed in George [7] where it was argued that real jets were intrinsically multilength scale phenomena since they add both mass and momentum at the source, and from these intrinsic length scale and velocity scales could be defined. For example, if ρm_o is the rate at which mass is added at the exit plane of the jet source, and ρM_o is the rate at which momentum is added, then the intrinsic length scale is

$$D_* = \frac{m_o}{M_o^{1/2}} \tag{8}$$

And the intrinsic velocity scale is given by

$$U_* = \frac{M_o}{m_o} \tag{9}$$

For a jet (which is driven by momentum), D_* provides a measure of how rapidly the mass added at the source is overwhelmed by that which is being continuously entrained as the flow evolves downstream. Thus, in effect, D_* and U_* provide the calibration against which development must be measured. Note that it was θ and U_∞ that played these roles for the wake considered above. The diameters of the wake generator themselves in fact varied greatly, even though the momentum thickness, θ, was held constant.

It is easy to show that if the exit profile is a top-hat and the jet diameter is D, then $D_* = \frac{\sqrt{\pi}}{2}D$ and $U_* = U_j$. Hence for a top-hat jet, D and U_j are the appropriate parameters to measure its development. But the important point of particular relevance here is that for any jet for which the exit profile is *not* a top-hat, the proper way to evaluate the effect of exit conditions is to compare plots of U/U_* versus y/D_*. Unfortunately, in at least some of the experiments earlier cited this was not done. Therefore some of the results might need to be reinterpreted. The exceptions are the experiments of Cater and Soria [36] and Shiri et al. [51], which will be discussed in detail below.

But before proceeding though, note that similar issues arise when buoyancy and swirl are added at the source. First consider buoyancy which is presumed to be added at the exit plane at a rate of ρF_o. This together with the rate at which momentum is added at the source, ρM_o, introduces another length scale, the so-called '*Morton*' length scale (Morton [52]) defined by

$$L_M = \frac{F_o^{3/4}}{M_o^{1/2}} \tag{10}$$

Just as D_* provides a measure of how fast a jet driven by momentum develops, L_M measures how rapidly a plume produces new momentum through buoyancy to overwhelm the rate at which momentum is added at the source. This can be very important in designing experiments and for interpreting results (see Kotsovinos and List [53], Baker et al. [54], Shabbir and George [55]).

Another length scale arises if there is swirl at the jet exit because of the angular momentum which is being added to the flow. If ρG_o is the rate at which angular momentum is being added, the corresponding swirl length scale is defined by Shiri et al. [51] as

$$L_s = \frac{G_o}{M_o} \tag{11}$$

Both linear and angular momentum must be conserved in the jet exiting into quiescent conditions, but the actual mean azimuthal velocity falls off more rapidly than that does the streamwise velocity (see Ewing [56]). As demonstrated below (and by Shiri et al. [51]), L_s provides a measure of the distance over which this happens and over which swirl appears to disappear. And the so-called "*swirl number*," $S = 2G_o/M_oD$, is just the ratio of this length scale to that over which the entrained mass dominates the rate at which mass was added initially. Clearly in light of the above, a more appropriate definition of swirl number would be

$$S_* = \sqrt{\pi}\frac{G_o}{M_o D_*} \tag{12}$$

where the factor of $\sqrt{\pi}$ has been added to make it reduce to the usual swirl number for top-hat jets.

The net effect of all three length scales, D_*, L_M, and L_s, is to displace the effective origin of the flow, (i.e., the virtual origin) and '*stretch*' it. As will be illustrated below for the swirling jet of Shiri et al. [51], failure to account for this shift can be misinterpreted as an extra (and extraneous) effect of source conditions on the growth rate and other development measures. The zero-mass-flux-jet is also of particular interest since it has no mass flux at all on the average ($m_o = 0$), but only an initial momentum, M_o. Thus it truly has only a single length scale, x, the distance downstream.

The Swirling Jet. The swirling jet experiments of Shiri et al. [51] provide an excellent example of the perils presented by *not* taking into account the considerations above when making comparisons. These experiments were conducted using burst-mode LDA at Chalmers in the relatively high Reynolds number (100,000) jet facility originally used by Hussein et al. [35], but the settling chamber was modified to introduce swirl using injectors in the manner of Gilchrist and Naughton [41]. Swirl at the jet exit has been known for some time to affect the initial development of the jet and enhance mixing (e.g., Chigier and Chervinsky [57], Farokhi et al. [58], Gilchrist and Naughton [41]). Therefore it was reasonable to assume that swirl was the perfect candidate to try to influence the far field as well. And indeed this appeared to be confirmed. The usual plots of jet half-width normalized by diameter, $\delta_{1/2}/D$, and maximum exit velocity normalized by the local centerline velocity, U_{max}/U, versus x/D showed a clear departure from the non-swirl case for the $S = 0.25$ experiment. We were worried a bit, however, about the exit velocity profiles shown in Fig. 20, which were slightly modified from their original very-near top-hat form by the swirl generator and the swirl itself.

So the exit profiles were carefully remeasured, and the parameters m_o, M_o, and G_o determined from them by integrating the appropriate profiles. Then the values of D_* and U_* (using Eqs. (8) and (9)) were computed for each experiment. Plots of $\delta_{1/2}/D_*$ and U_*/U_c versus x/D_* are shown in Figs. 21 and 22. Clearly, and to our considerable surprise, there were no significant differences in the asymptotic spreading or the centerline decay rates. Only the virtual origin was shifted for the $S = 0.25$ case.

Figure 23 shows the normalized mean velocity profiles for all three experiments. These results are as expected, since even if source conditions mattered these profiles should be identical from the equilibrium similarity arguments (see Ewing [56], see also Shiri et al. [51]). Consistent with the spreading rates and centerline velocity decay was that the turbulence intensities also showed little difference except for the downstream distance required for development as shown in Fig. 24. In fact, all other velocity moments were nearly indistinguishable from each other, and as well from those of Hussein et al. [35]. Subsequent experiments reported by Shiri et al. [59,60] measuring moments to the fourth order also showed no effect of swirl.

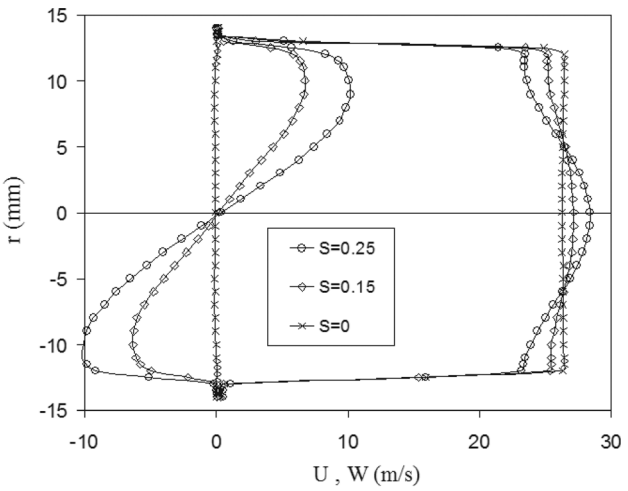

Fig. 20 Axial (rightmost) and tangential (leftmost) velocity profiles for swirling jet at the jet exit at three different swirl number ($S = 0$, 0.15, and 0.25)

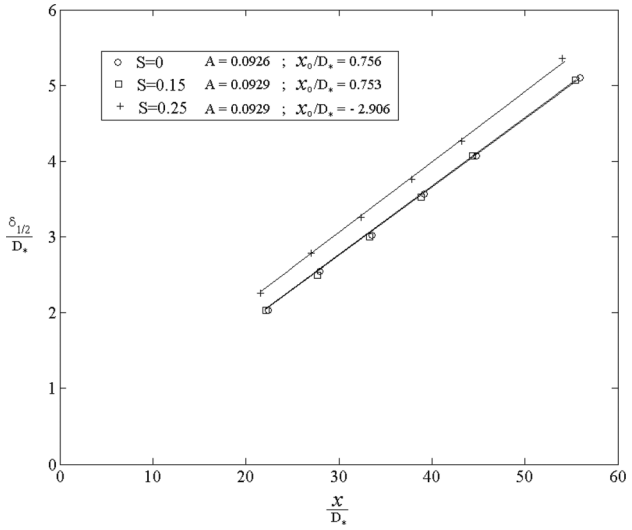

Fig. 21 Streamwise variation of the half-width for swirling jet experiments plotted as $\delta_{1/2}/D_*$ versus x/D_*

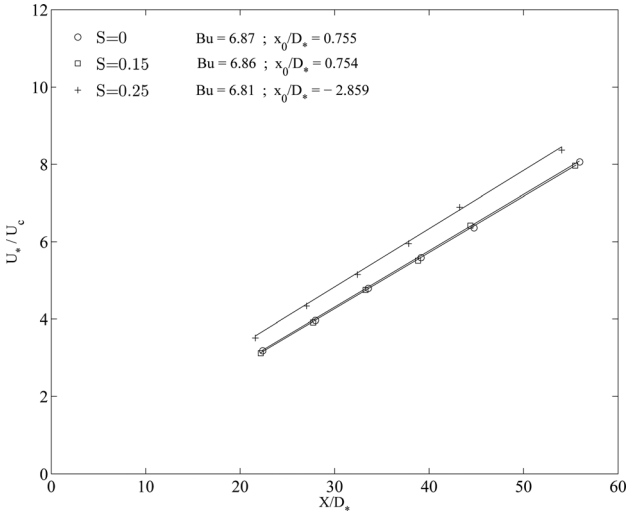

Fig. 22 Streamwise variation of centerline mean velocity for swirling jet experiments plotted as U_*/U_c versus x/D_*

The Zero-Net-Mass-Flux Jet. As is clear from the photographs of Fig. 19 there are in fact real differences between the zero-net-mass-flux jet and the steady jet. The experiments were carried out using PIV at Monash University by Cater and Soria [36] using a pulsed jet created with a piston, so that positive parts the cycle very closely balanced the negative part of the cycle. But even though there was no net mass added to the flow over a cycle, there was a source of momentum since negative momentum going backwards has the same sign as positive momentum going forwards. They summarized their results as follows:

> "In summary, the reason that zero-net-mass-flux (ZNMF) jets spread differently throughout the domain is due to structural differences in the near field. Although, the shape of the mean velocity profiles is similar to a continuous jet in the far field, the mean streamwise gradients are different…This leads to the non-universality of constants in similarity solutions for turbulent jets across different velocity profiles, as well as the source Strouhal number dependence of the jet statistics" (From Cater and Soria [36]).

Plots of the downstream development of the jet half-width and profiles of mean velocity are shown in Figs. 25 and 26.

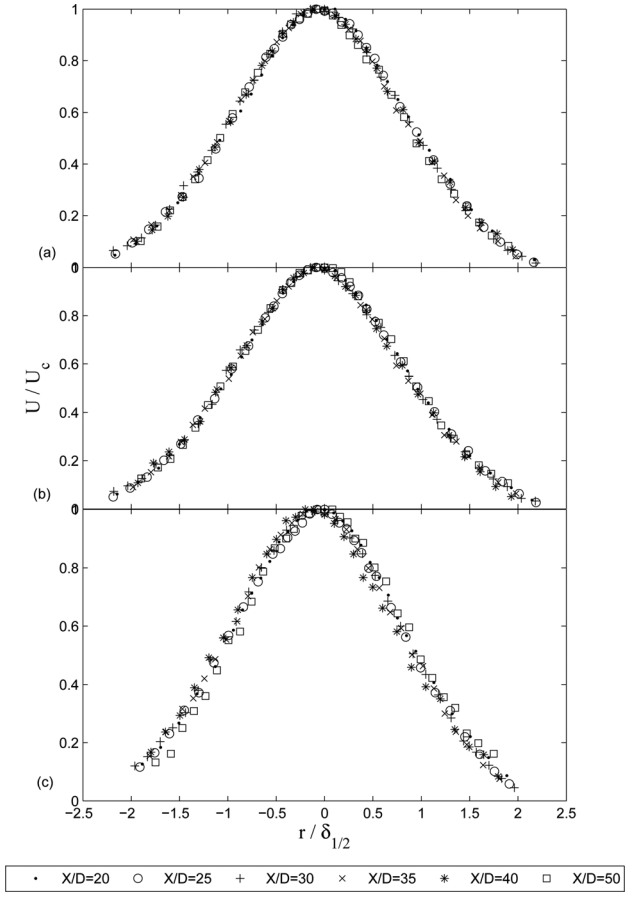

Fig. 23 Mean stream-wise velocity profiles for swirling jet experiments at different axial position for the three different cases: (*a*) S = 0, (*b*) S = 0.15, (*c*) S = 0.25. The profiles have been normalized by the local mean centerline velocity, U_c, and the half-width, $\delta_{1/2}$.

The ZNMF jet half-width spreads about 30% faster than the steady jet, and the corresponding velocity profile is considerably wider. At first glance, this appears to violate the equilibrium similarity argument that the mean velocity profiles should be the same, but it does not. The velocity profile was not plotted by the authors as a function of $r/\delta_{1/2}$ but instead as a function of r/x, thus emphasizing the actual physical spread of the jet. Figure 27 shows profiles of the streamwise component of the Reynolds stress normalized by the square of the centerline velocity (square of turbulence intensity), and compares it to other jets. Clearly the pulsed jet turbulence intensities are substantially higher, as might have been expected given its pulsatile nature.

Nonstationary Homogeneous Turbulence

Background. To this point all of the free shear flows we have considered have been stationary random processes (i.e., statistics independent of origin in time), but inhomogeneous in at least one space dimension. Now we consider the opposite: flows that are nonstationary so their statistics change with time, but are homogeneous in space. Homogeneous turbulence may seem even more esoteric for engineers than the free shear flows discussed earlier in this article. Yet many of our ideas about the dynamics of turbulence started with these flows, and all of the engineering turbulence models depend on them. The simplest example is the familiar relationship used in all models in one form or another, $\varepsilon \propto u^3/L$, where ε is the rate at which turbulence energy, $3u^2/2$, is dissipated and L is presumed to bear some relation to the integral scale. Not only is it often assumed that this relationship is valid, it

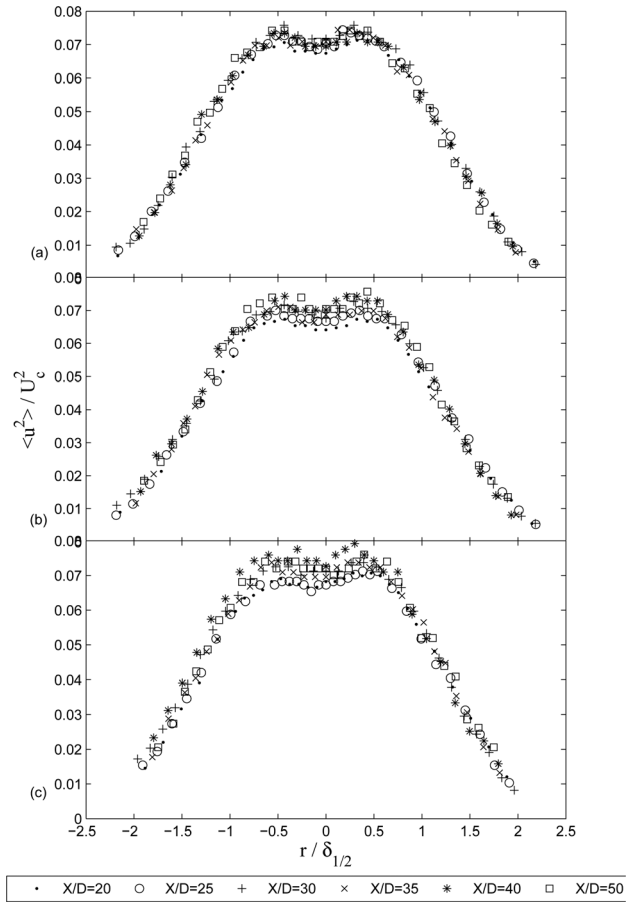

Fig. 24 RMS stream-wise velocity for the swirling jet experiments at different axial position for the three different cases: (*a*) S = 0, (*b*) S = 0.15, (*c*) S = 0.25. The profiles have been normalized by the local mean centerline velocity, U_c, and the half-width, $\delta_{1/2}$.

is often also assumed the coefficient of proportionality is universal. It is easy to see from one of the flows we considered earlier that this cannot be true in general. Consider this: the integral scale can be shown to be proportional to the value of the one-dimensional spectrum divided by the energy u^2 in the limit as the wavenumber goes to zero. The spectra of the time-dependent wake shown earlier (Figs. 7–10), however, showed the lowest

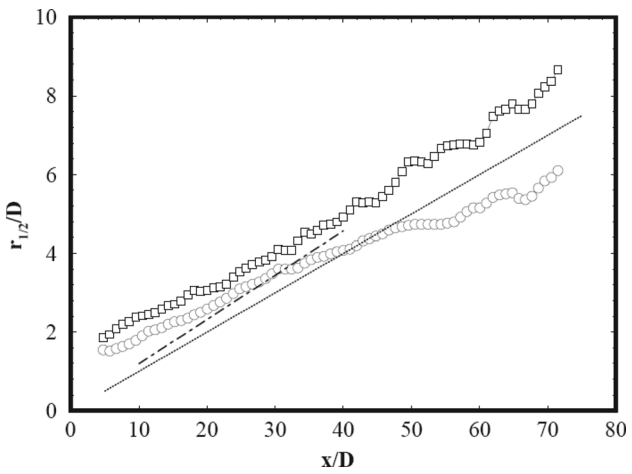

Fig. 25 Half-widths normalized by jet exit diameter versus x/D for the ZNMF jet (squares) and steady jet (circles), compared to that of Hussein et al. [35](- - -) from Cater and Soria [36]

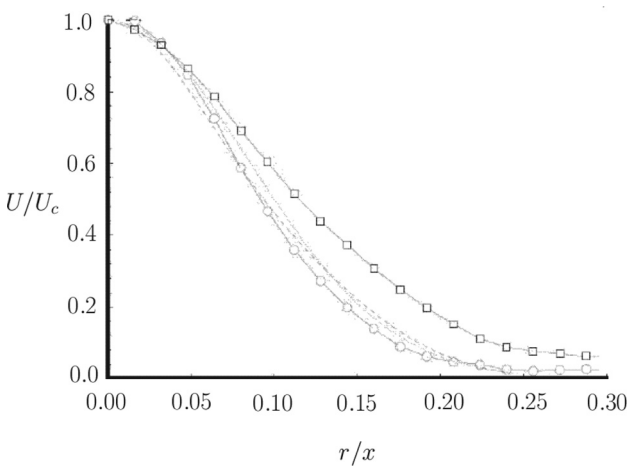

Fig. 26 Mean velocity profiles from ZNMF jet (squares) and steady jet (circles) normalized by centerline velocity, from Cater and Soria [36]. Solid line is from pulsed jet of Bremhorst et al. [61]. Dashed line is typical steady jet.

(and most energetic) values of the spectrum to have been the most influenced by the initial conditions. The highest wavenumbers which dominate the dissipation, however, were minimally influenced by the initial conditions. Thus the ratio, $\varepsilon L/u^3$, must also depend on the upstream conditions. The point is that once we open the Pandora's box of possible dependence on upstream conditions, much of what we have believed to be true about turbulence must be seen to be as at best an approximation. Nowhere, it seems, is this more true than for nonstationary homogeneous turbulence.

The oldest example of an nonstationary homogeneous turbulence is simply turbulence which decays in the absence of all spatial gradients of mean quantities. An experimental approximation to this homogeneous decaying turbulence is the turbulence generated downstream of a grid in a wind tunnel. Because of the low turbulence intensity (and the negligibility of the streamwise turbulence transport terms), Taylor's frozen field hypothesis can be invoked locally so that time, t, can replaced by distance downstream divided by the tunnel speed, x/U. The early measurements of Batchelor and Townsend [62] seemed to confirm the von Karman and Howarth [63] theory of self-preservation in which the energy decayed as $u^2 \propto t^{-1}$. But almost none of the other experiments could replicate these results; and it was this problem that was a major reason for the construction of what is now referred to

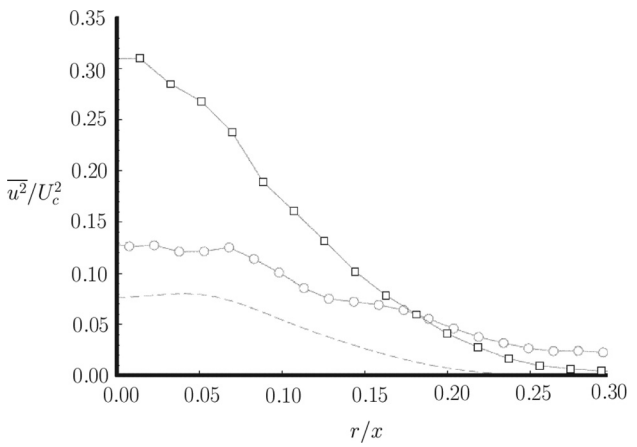

Fig. 27 Streamwise component of Reynolds stress from ZNMF jet at two different Strouhal numbers, 0.00072 (squares) and 0.0015 (circles) compared to that of Hussein et al. [35] (- - -), from Cater and Soria [36]

as the Corrsin Wind Tunnel at the Johns Hopkins University. Using this tunnel, Comte-Bellot and Corrsin carried out an extensive series of experiments which are reported in Refs. [14,15]. They also summarized the results of the experiments of others prior to 1966. With a single exception, none of the results showed the turbulence decaying as t^{-1}, but in fact as a noninteger power of time: $u^2 \propto t^n$ where $n < -1$ (the exception was the Kistler and Vrebalovich [64] experiment which was carried out in a wind tunnel that was destroyed immediately thereafter, so the results could never be confirmed). To this day, it seems to be commonly believed that the Comte-Bellot and Corrsin experiments produced a single universal value for the decay parameters, usually something near $n \approx -1.28$. But in reality it was only for the square bar grids that this result was achieved. In fact values of n varied from about -1.1 to -1.5, depending on the precise geometry of the grid and the tunnel speed. The mythology of a universal value of n seems to have been fed as much by desires of the turbulence community for universality as by the data, and especially by the turbulence modelers who at least in the 1970s and 1980s were still hoping for universal modeling constants (note that their C_{ε_1}, in particular, is directly determined by n, since power law decay implies that $C_{\varepsilon_1} = (n-1)/n$, see Reynolds [65]). As a consequence, experimentalists (using both laboratory and DNS) have continued to search for the elusive universal value of n, hoping eventually to find that it does not depend on the upstream conditions. There has, however, been considerable debate as to how and whether it is influenced by the degree of anisotropy present. And there has even been debate about whether n itself varies during decay as a function of the *local* Reynolds number.

My own special interest in decaying turbulence began in the spring of 1987 when I was teaching a second advanced turbulence course at the State University of New York at Buffalo. As we discussed the von Karman and Howarth self-preservation theory for decaying isotropic turbulence, one of the students, (James Sonnenmeier) who had been in the aforementioned earlier class the semester before remarked, "Are we going to disprove this theory too?" Almost simultaneously everyone at the table realized that it had indeed been over-constrained as well.

Here is the crux of the arguments first published in George [7] (see George [11] for a more comprehensive presentation). Begin with the spectral energy equation for decaying homogeneous turbulence given by

$$\frac{\partial E}{\partial t} = T - 2\nu k^2 E \tag{13}$$

where $E(k,t)$ is the three-dimensional energy spectrum function, $T(k,t)$ represents the nonlinear transfer processes removing or adding energy at a given wavenumber, k, and ν is the kinematic viscosity (v. Batchelor [66], Tennekes and Lumley [6], Monin and Yaglom [67]. $E(k,t)$ has been obtained by integrating the three-dimensional spectrum over spherical shells of radius $k = |\vec{k}|$, which has in turn been obtained by taking the three-dimensional transform of the two-point velocity correlation tensor (it is a common misconception that this equation is only valid for isotropic turbulence, but in fact only homogeneity is required).

The nonlinear spectral transfer term $T(k,t)$, is deceptively simple, but accounts for the net effect of all the nonlinearity of the Navier-Stokes equations. For homogeneous turbulence these can be characterized as being entirely due to interactions among triads of wavenumbers, say $\vec{k}, \vec{k'}$ and $\vec{k''} = \vec{k'} - \vec{k}$ as illustrated in Fig. 28.

It is the interactions of wavenumbers that are nearly of the same size which dominate the energetics of the turbulence. And at high Reynolds numbers, it is these interactions among wavenumbers of nearly the same size in the range of wavenumbers that are larger than those containing most of the energy yet still smaller than those doing most of the dissipation that are largely responsible for what is often referred to as the 'energy cascade.' As noted by Ref. [6] (see also Ref. [68]), however, this 'cascade' is at best a rather 'leaky one'.

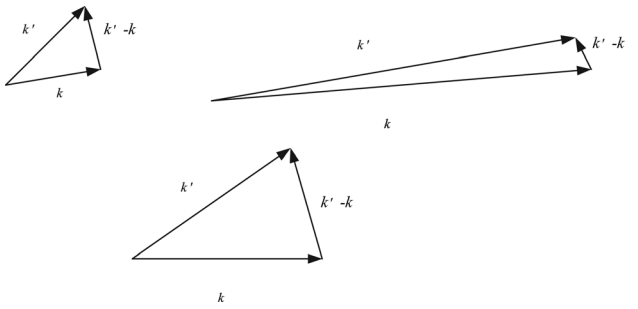

Fig. 28 Sketches illustrating three of the triply infinite number of nonlinear triadic interactions that comprise homogeneous turbulence

While quite useful for theoretical analysis, $E(k,t)$ can almost never be obtained experimentally[4]. Nonetheless, with the assumption of isotropy (v. Ref. [67].), $E(k,t)$ can be related to the more accessible whole-line one-dimensional streamwise velocity spectrum, $F_{1,1}^{(1)}$ (or $F_{2,2}^{(1)}$) by

$$E(k,t) = k^3 \frac{\partial}{\partial k}\left[\frac{1}{k}\frac{\partial F_{1,1}^{(1)}(k,t)}{\partial k}\right] \tag{14}$$

$$= k^2 \frac{\partial^2 F_{2,2}^{(1)}(k,t)}{\partial^2 k} - k\frac{\partial F_{1,1}^{(1)}(k,t)}{\partial k} \tag{15}$$

where

$$F_{1,1}^{(1)}(k_1) = \frac{1}{2\pi}\int_{-\infty}^{\infty} e^{-k_1 r}\langle u_1(x_1,x_2,x_3)u_1(x_1+r,x_2,x_3)\rangle dr$$
$$= \frac{1}{2}\int_{k_1}^{\infty}\frac{E(k,t)}{k^3}[k^2 - k_1^2]dk \tag{16}$$

$$F_{2,2}^{(1)}(k_1) = \frac{1}{2\pi}\int_{-\infty}^{\infty} e^{-k_1 r}\langle u_2(x_1,x_2,x_3)u_2(x_1+r,x_2,x_3)\rangle dr$$
$$= \frac{1}{4}\int_{k_1}^{\infty}\frac{E(k,t)}{k^3}[k^2 + k_1^2]dk \tag{17}$$

Note that the subscripts on the one-dimensional spectra indicate the velocity components, while the superscript indicates the direction over which the corresponding two-point correlation functions are measured (e.g., $\langle u_1(x,y,z,t)u_1(x+r,y,z)\rangle$ or $\langle u_2(x,y,z,t)u_2(x+r,y,z)\rangle$, or equivalently, the components of the three-dimensional spectrum in vector space, (k_1,k_2,k_3) which are *not* integrated over to produce it.

The integral of $E(k,t)$ overall wavenumbers is the turbulence kinetic energy; i.e.,

$$\frac{1}{2}\langle u_i u_i\rangle = \frac{3}{2}v^2 = \int_0^{\infty} E(k,t)dk \tag{18}$$

while the integral of the one-dimensional spectra over the whole line yields only the component variances; i.e.,

$$\langle u_\alpha^2\rangle = \int_{-\infty}^{\infty} F_{\alpha,\alpha}^{(1)}(k_1,t)dk_1 \tag{19}$$

where there is no summation on α.

Also the integral of $2\nu E(k,t)$ is the rate of energy dissipation per unit mass, ε; i.e.,

[4]The exception to this are DNS results which can be thought of as numerical experiments. More will be said on this later.

$$\varepsilon = 2\nu \int_0^\infty k^2 E(k,t) dk \tag{20}$$

which, if one can assume isotropy, corresponds to

$$\varepsilon = 15\nu \int_{-\infty}^{\infty} k_1^2 F_{1,1,}^{(1)}(k_1,t) dk = 15\nu \left\langle \left[\frac{\partial u_1}{\partial x_1}\right]^2 \right\rangle \tag{21}$$

Note that ε is often called simply the *dissipation*. Similar equivalences can be derived for any quantity derivable from either the three-dimensional spectrum function, $E(k,t)$, or the one-dimensional spectra, but again with the assumption of isotropy. It is this fact that in part explains what some engineers might describe as the 'fixation' of the turbulence community on isotropic flows: without this assumption we have only very limited tools to compare theory to experiment.

Thus any theoretical deduction or scaling law derived for the three-dimensional energy spectrum function, $E(k,t)$ can readily be applied to the one-dimensional spectra, at least with the assumption of isotropy. One confusing and misleading feature of the one-dimensional spectra, however, is that they do not go to zero for low wavenumbers, but (as noted above) are in fact proportional in the limit as $k_1 \to 0$ to the product of the component energy and the integral scale, v. Ref. [6]. Another is that any filtering applied to one direction (say by finite probe size) shows up not just at large wavenumbers (or frequencies) but at all, v. Ref. [69].[5] Both of these effects are because of the aliasing of information from the other two directions, say k_2 and k_3 into the k_1 direction. In spite of these annoying features, in the absence of good alternatives, one-dimensional spectra remain a primary tool for experimentalists.

Now back to our immediate problem: the basic idea is to again seek an equilibrium similarity solution to Eq. (13). First transform the equations by seeking solutions of the form

$$E(k,t) = E_s(t,*)F(\overline{k},*) \tag{22}$$

$$T(k,t) = T_s(t,*)G(\overline{k},*) \tag{23}$$

where $\overline{k} = kL(t)$. The scaling functions, $E_s(t,*)$, $T_s(t,*)$, and the length scale, $L(t,*)$, are functions of time and initial conditions only, and cannot be specified arbitrarily but must be determined from the equilibrium similarity hypothesis. The dimensionless spectrum, $F(\overline{k},*)$, and spectral transfer function, $G(\overline{k},*)$, are functions of only the nondimensional wavenumber, $\overline{k}$ and any residual initial conditions effects denoted by *. Applying the chain-rule and substituting into the spectral energy equation yields

$$\left[\frac{dE_s}{dt}\right]F + \left[\frac{E_s}{L}\frac{dL}{dt}\right]\overline{k}F' = [T_s]G - 2\left[\frac{\nu E_s}{L^2}\right]\overline{k}^2 F \tag{24}$$

where the $'$ denotes differentiation with respect to $\overline{k}$. Thus, we have achieved a separation of variables in which all of the explicit time-dependence is in the square-bracketed terms, and all of the dependence on dimensionless wavenumber is outside of them.

It is here that the equilibrium similarity hypothesis is invoked: we ask whether solutions can exist for which all the bracketed terms have the same time dependence. And in fact there are *if* the following conditions can be satisfied

$$\left[\left(\frac{1}{\nu L}\right)\frac{dL}{dt}\right] = A \tag{25}$$

$$\left[\left(\frac{L^2}{\nu E_s}\right)\frac{dE_s}{dt}\right] = B \tag{26}$$

$$\left[\frac{L^2 T_s}{\nu E_s}\right] = C \tag{27}$$

where $A = A(*)$, $B = B(*)$ and $C = C(*)$ are at most constants that depend on the initial conditions.

It is easy to show by substitution into the energy and dissipation integrals that the length scale, L, can be taken equal to the longitudinal integral scale, L_{11}, defined from the longitudinal streamwise correlation, $B_{LL}(r) = \langle u(x,y,z,t)u(x+r,y,z,t)\rangle$, as

$$L_{11} = \frac{1}{\langle u_1^2\rangle}\int_0^\infty B_{LL}(r)dr = \lim_{k_1\to 0}\frac{\pi}{\langle u_1^2\rangle}F_{1,1}^{(1)}(k_1) \tag{28}$$

Or equivalently for isotropic turbulence from $E(k,t)$ it is given by

$$L_{11} = \frac{\pi}{2v^2}\int_0^\infty \frac{E(k,t)}{k}dk \tag{29}$$

Alternatively L can be taken equal to the Taylor microscale, λ, defined by

$$\lambda^2 = 15\nu\frac{v^2}{\varepsilon} \tag{30}$$

Whichever is chosen is irrelevant from a theoretical perspective, since the consequences of equilibrium similarity demand they remain proportional during decay. In fact, it is this constant ratio, L_{11}/λ, during decay that is most representative of the real Reynolds number characterizing the turbulence. As a practical matter, the better choice is usually λ since it is less influenced by the finite boundaries of experiments and simulations (v. Wang and George [70]).

The scale functions, $E_s(t,*)$ and $T_s(t,*)$, can now be determined without loss of generality to be

$$E_s(t,*) = v^2\lambda \tag{31}$$

$$T_s(t,*) = \frac{\nu v^2}{\lambda} \tag{32}$$

It follows immediately from the conditions for equilibrium similarity that the turbulence can be *deduced* to decay as a power law in time; i.e.,

$$\frac{v^2}{v_{\text{ref}}^2} = \left(\frac{t-t_o}{t_{\text{ref}}-t_o}\right)^n \tag{33}$$

where t_o represents a virtual origin, and the exponent, $n = n(*)$, is a negative constant and at most a function of the initial conditions. Note that prior to this result, Eq. (33) was always believed to be an empirical law, at least for $n \neq -1$. Clearly this is not the case.

To say that these ideas were less than enthusiastically received by the turbulence community would be an understatement[6]. There were indeed some legitimate concerns about how well the theory described all features of the experimental and DNS data, some of which are still being debated and researched today. The new theory was, on the other hand, able to make some remarkable predictions consistent with the observations, including a power law decay with the decay exponent different from -1 and dependent on the initial (or upstream) conditions. Most of these were presented in detail in George [11].

But the real problem presented by the work was that it challenged much of what the turbulence community had come to believe about turbulence in the preceding four decades, in part because of the well-documented failures of the von Karman and Howarth self-preservation theory for decay [63,67,71]. In particular:

[5]These effects are commonly hidden by plotting the so-called 'pre-multiplied' spectra, which are obtained by multiplying the one-dimensional spectra by wavenumber.

[6]The paper finally published as George [11] was resubmitted 8 times and reviewed 26 times before being ultimately published in 1992.

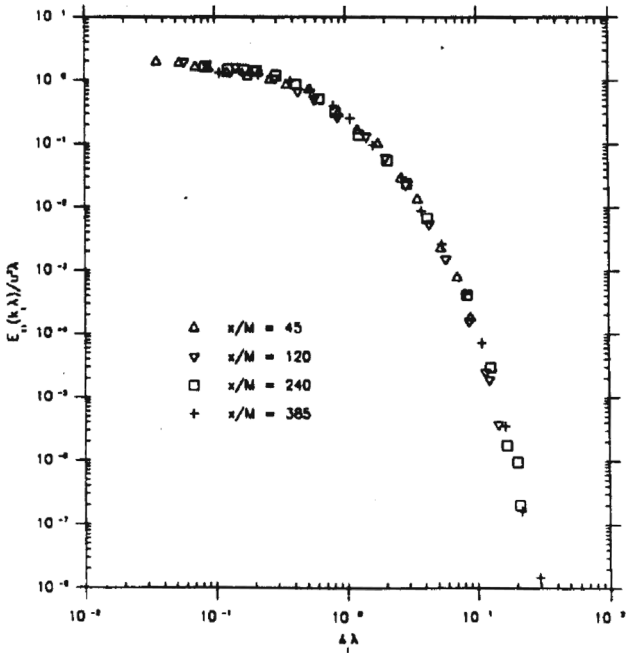

Fig. 29 One-dimensional streamwise velocity spectra downstream of one-inch square bar grid at 10 m/s in 10 m length Corrsin wind tunnel plotted in Taylor variables for all downstream positions. Data of Comte-Bellot and Corrsin [15].

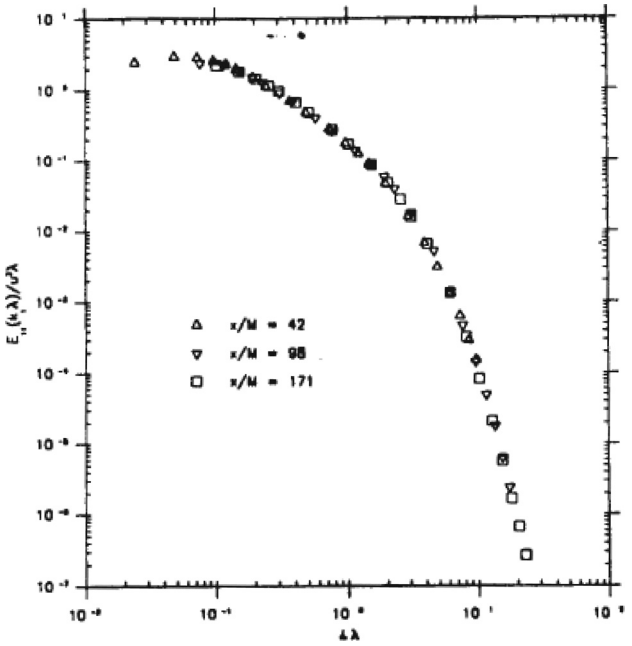

Fig. 30 One-dimensional streamwise velocity spectra downstream of two-inch square bar grid at 10 m/s in 10 m length Corrsin wind tunnel plotted in Taylor variables for all downstream positions. Data of Comte-Bellot and Corrsin [15].

First, the new theory argued that initial conditions might be (and probably were) important for decaying turbulence, contrary to what had long been believed.

Second, it declared that at least some turbulence could be described by a single length scale, contrary to all conventional wisdom since Batchelor [71].

Third, it argued that in fact the appropriate length scale was the Taylor microscale. As shown in Figs. 29 and 30, the well-established one-dimensional spectral data of Comte-Bellot and Corrsin [15] plotted in Taylor variables collapsed at all scales quite spectacularly, and to different curves for different initial (or upstream) conditions. Nonetheless, this was contrary to all thinking at the time which believed that the Taylor microscale could only be interpreted as a time scale (in conjunction with the turbulence intensity), see, for example, Tennekes and Lumley [6].

Fourth, it argued that the derivative skewness (which measures the production of dissipation and mean square vorticity) *increased* during decay as the local Reynolds number decreased, and in fact was predicted to vary inversely with R_λ. This was contrary to the usual assumption since Batchelor and Townsend [72] that the derivative skewness was constant during decay, in spite of considerable evidence to the contrary that it increased (e.g. Refs. [62,73–75]. As a case in point, some of this data is replotted in Fig. 31. The theory also *appeared* to contradict all the arguments for increasing internal intermittency with increasing Reynolds number (e.g., Ref. [76]), which would cause the opposite effect. Note that this is only an apparent contradiction: in fact, both arguments can be true since intermittency can increase with L_{11}/λ (i.e., with increasing Reynolds number of the initial conditions) *as well as* during decay for fixed initial conditions. Thus, neither R_λ nor L_{11}/λ uniquely characterize the state of the turbulence, only both together. But even this invalidated the long-standing practice in turbulence (even today) to cite only R_λ.

Fifth, the idea stemming from Kolmogorov [77] that $\varepsilon L_{11}/v^3$ was a constant in decaying turbulence was challenged. The reason for the conflict is easy to see: If L_{11}/λ is constant during decay (as the new theory deduces) and by definition $\lambda^2 = 15\nu u^2/\varepsilon$, then the only way u^3/ε could be proportional to L_{11} were if $R_\lambda = constant$ during decay. But since for any power law decay $\lambda^2 \propto t$ (v. Ref. [66].), R_λ could be constant throughout decay only if u^2 were inversely proportional to time–which it most certainly seemed from almost all available evidence not to be. Challenging $\varepsilon \propto u^3/L_{11}$ (even for a very special flows) was, of course, considered heresy of the highest degree, even challenging whether the coefficient were universal.

Finally, and more problematically at the time, even though the experiments in most wind tunnels seemed to be in agreement with the predictions, the DNS of decaying turbulence (at that time in its infancy) did not seem to behave like the equilibrium similarity theory suggested.

By contrast with DNS, however, and in support of the new equilibrium similarity approach, application of the same methodology to other homogeneous nonstationary flows accounted well for the existing experimental results, some of which had been quite puzzling. For example, as shown in Figs. 32 and 33, the predictions for decaying grid turbulence with temperature and velocity fluctuations seemed to be in excellent agreement with the surprising experimental results of [16], especially the prediction of the role of initial conditions and the Taylor spectral scaling [12]. Similarly, as illustrated in Figs. 34–36, the equilibrium similarity analysis by George and Gibson [13] accurately predicted the growing consensus about homogeneous shear flow turbulence: namely its dependence on initial (or upstream) conditions, and that the turbulence intensity grew exponentially with time while the Taylor microscale appeared to be asymptotically constant (e.g., Rohr et al. [17], Tavoularis and Karnik [78], Gibson and Kanellopoulos [18]). Moreover, it predicted the hitherto unnoticed collapse of the velocity spectra in Taylor variables.

But in spite of these successes, the apparent disagreement with the DNS, especially for decaying turbulence, pretty much kept the new theory in limbo, at least through most of the 1990s. And there in limbo with it was any discussion of the role of initial conditions in decaying turbulence. How we got from there to the present provides an interesting insight into both the purely technical

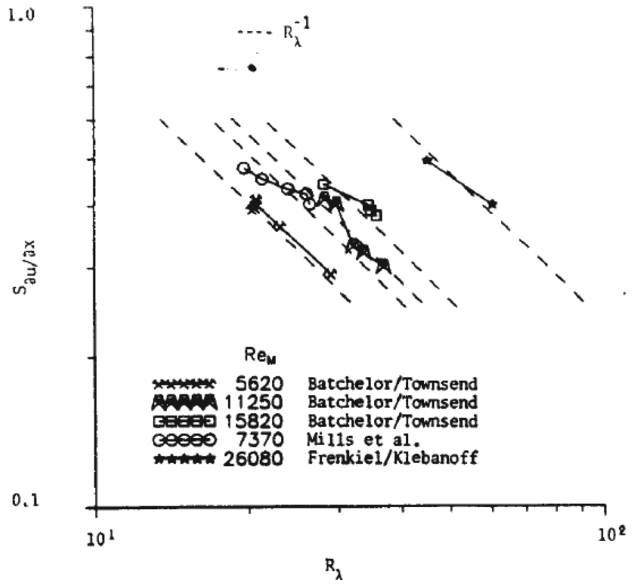

Fig. 31 Log-log plot of derivative skewness of Batchelor and Townsend [62], Mills et al. [73] and Frenkiel and Klebanoff [74] plotted versus R_λ. Dotted lines correspond to $S_{\partial u/\partial x}$ $R_\lambda = constant$ for fixed upstream conditions, each of which denotes different grid and grid Reynolds number (from [11]).

difficulties of doing good turbulence research, and how science progresses. Ultimately the real test of any new theory is whether it can predict something previously never observed, and we shall see that happened as well.

Understanding the DNS. DNS (or Direct Numerical Simulation) represents one of the great intellectual triumphs of the 20th Century, and in one sense the ultimate triumph for fluid dynamicists. Finally, we can directly calculate solutions to the Navier-Stokes equations that look like flows we observe in nature. These are equations we generally are incapable of solving analytically for turbulence problems. Moreover we have more or less complete control over boundary conditions and initial conditions, and can ask questions experimentalists and fluid dynamicists of previous generations could have never imagined getting answers to. The ability to do DNS, however, has not come easily, and is still very much a work in progress, in part because as computers increase in size we can do more complex and larger computations. However, in greater part because in the absence of any analytical solutions

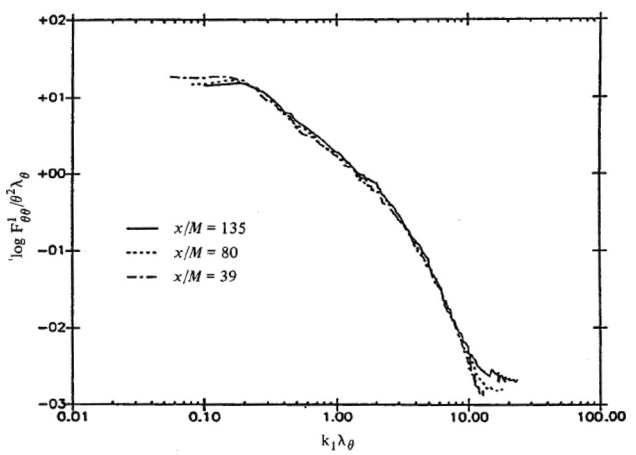

Fig. 32 One-dimensional temperature spectra downstream of a grid in Taylor variables. Data of Warhaft and Lumley [16] (from Ref. [12]).

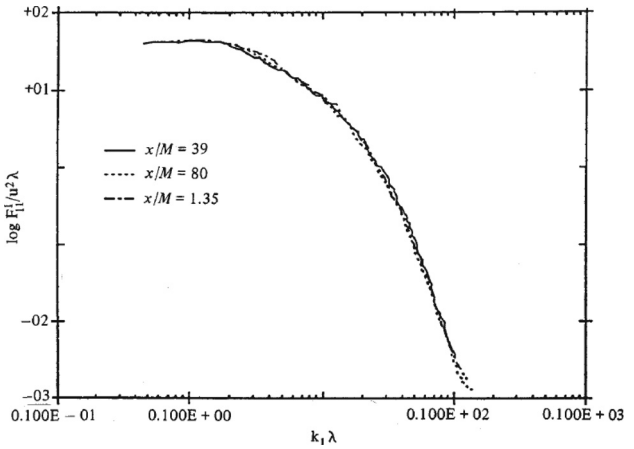

Fig. 33 One-dimensional velocity spectra behind grid in Taylor variables. Data of Warhaft and Lumley [16] (from Ref. [12]).

for turbulence, there has been no real test for whether the simulations were done correctly.

The first clue that there might be a problem with the DNS and not the equilibrium similarity theory solution came in fact to me from one of the pioneers of DNS for decaying turbulence (Jim Riley of the University of Washington), who made the passing comment to me at an APS meeting in the early 1990s that DNS turbulence (at least at that time) did not quite look like real grid turbulence. The second clue came during a stay in early 1999 at

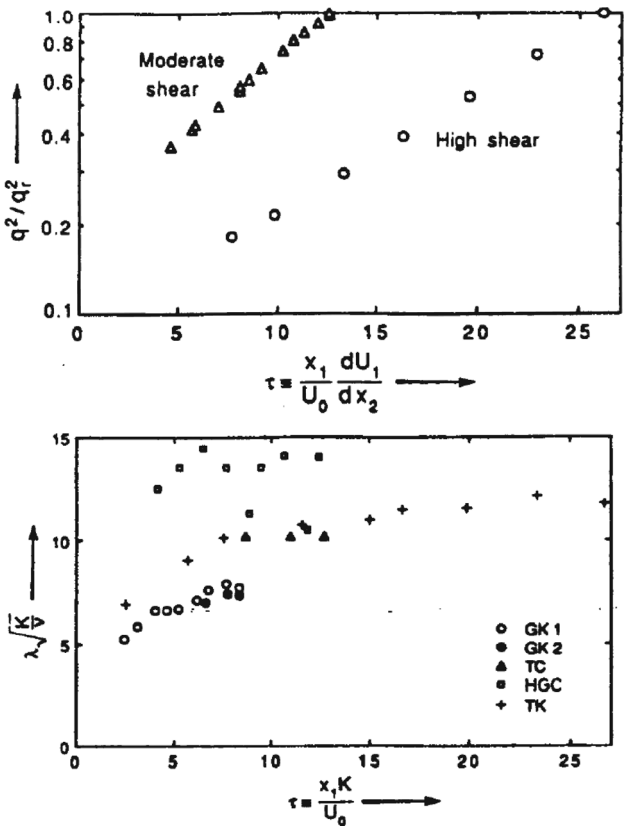

Fig. 34 upper: Semi-log plot of turbulence intensities of Tavoularis [79] showing clearly exponential growth. Lower: Taylor microscales reach constant asymptote determined by initial (upstream) conditions. Data of Gibson and Kanellopoulos [GK1, GK2] [18]; Tavoularis and Corrsin [TC] [80]; Harris, Graham, and Corrsin[HCG] [81], and Tavoularis and Karnik [TK] [78]. From Ref. [13].

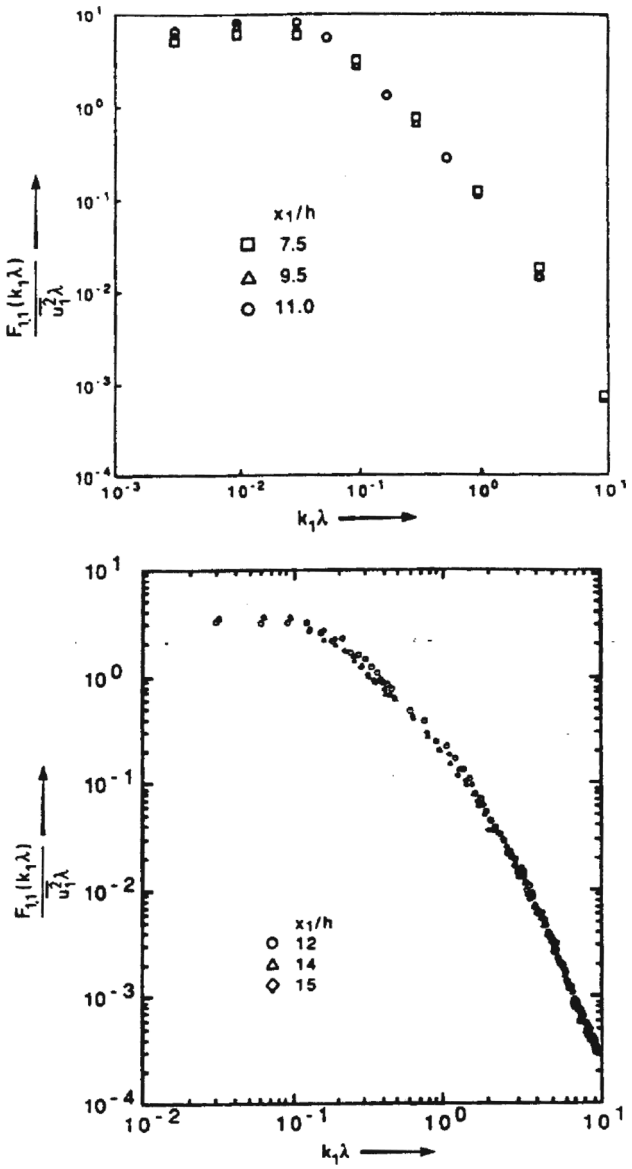

Fig. 35 One-dimensional velocity spectra from two different homogeneous shear flow experiments collapsed in Taylor variables. Upper: Tavoularis and Corrsin [80]; lower: Gibson and Kanellopoulous [18]. Each experiment has a unique spectral shape, reflecting the different mean shear rates and upstream conditions. From Ref. [13].

the Isaac Newton Institute for Mathematics at Cambridge University in the UK at a special program on turbulence sponsored by the Royal Engineering Academy. While examining some recent DNS with Jack Herring of NCAR and David McComb of the University of Edinburgh, they enlightened me as to some of the tricks used and difficulties of carrying out such large scale simulations. For example, *averaging* for nonstationary problems is not really *averaging* in the normal sense that we would think of for a stationary random process. It almost always performed over space or wavenumber at any given time for only one member of an ensemble. And this works only if the initial phases are carefully randomized to remove at least some of the effects of the initial conditions. Moreover, as in any experiment, the initial conditions very much determine the solution. At first glance, this would seem to be consistent with the ideas presented herein, except for the initial randomization. Much more important it turns out is how close the simulated flow is (or is not) to representing a homogeneous flow in an infinite enviroment.

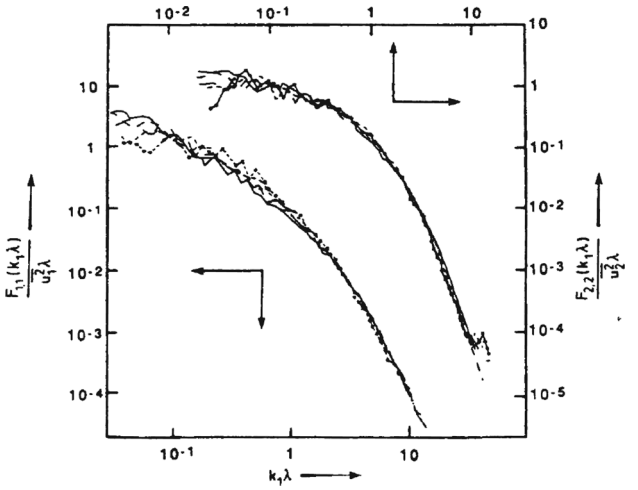

Fig. 36 Streamwise and cross-stream one-dimensional velocity spectra in Taylor variables from homogeneous shear flow experiments of Rohr et al. [17]. Note excellent collapse at all wavenumbers except for the very lowest which are larger than the tunnel width so clearly cannot be considered representative of homogeneous flow. From Ref. [13].

When I returned to the State University of New York at Buffalo, I immediately set out in cooperation with a Ph.D. student, Stephan Gamard, and post-doc, Honglu Wang, to examine the simulations produced by some of our colleagues at Buffalo. To my surprise, it seemed that a common practice by at least some in the field was to set the peak in the energy spectrum as close to the lowest wavenumber as possible in order to get the highest possible Reynolds number. So close in fact that the turbulence had little chance of approximating a homogeneous turbulence, but instead was more like turbulence in a box—which in fact it was! By utilizing two carefully performed 512^3 simulations which did *not* make this mistake, one from Alan Wray [82] and another from Steve de Bruyn Kops and Jim Riley [83], we were able to make the case that in fact the equilibrium similarity provided at least a reasonable description of these simulations. Figures 37 and 38 show the spectral data from both these simulations plotted in Taylor variables.

Moreover, we were able to identify the departures from equilibrium similarity with specific limitations of the simulations themselves (e.g., box size, ratio of integral scale to box-size, high wavenumber cutoff, etc.), all detailed in Wang et al. [84]. The 32^3 simulations subsequently performed in 2001 with my new colleagues at Chalmers, Christian Wollblad and T. Gunnar Johansson, confirmed in a systematic way our suspicions about the effect of box-size; in particular, that it significantly deteriorated the collapse of the spectra in Taylor variables. They also proposed an unambiguous way using $d\lambda^2/dt$ (discussed briefly below) for identifying what the decay power exponent was quite independent of any virtual origin in time. All these efforts were summarized the paper by George et al. [85] at the Australasian Fluid Mechanics meeting in a session chaired by Bob Antonia of the University of Newcastle. After that, it seemed Bob and his co-workers went on a mission to evaluate and prove (or disprove) the equilibrium similarity theory. As a consequence, much of the actual progress in this field has come from Australia, with me just along for the very exciting ride as interested observer. Another set of key players to recently enter the theater is the team headed by Christos Vassilicos at Imperial College of London using fractal grids. I shall attempt in the following paragraphs to summarize what I think has happened in the last decade, where I think things now stand, and what outstanding issues are left to be resolved.

Does the Decay Rate Really Depend On The Initial Conditions? It is easy to show (Batchelor [66]) that an immediate consequence of any power law decay is that the square of the

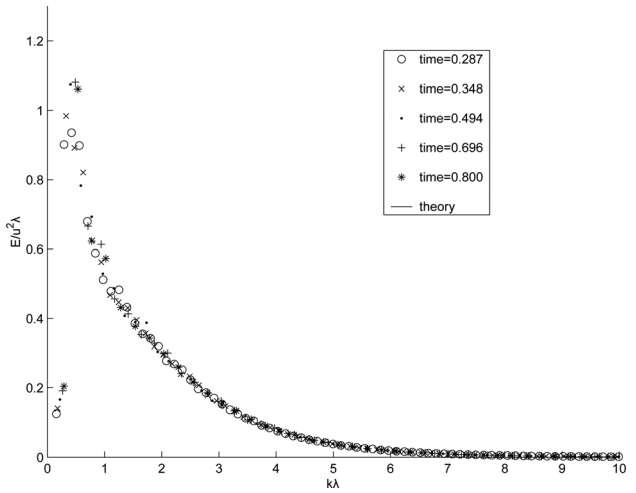

Fig. 37 Three-dimensional energy spectrum function, $E(k,t)$ plotted in Taylor variables using DNS data of deBruyn Kops and Riley [83], from Wang and George [70]. Note that unscaled data varied by approximately a factor of 8 for the time segment shown. Also note the sparseness of low wavenumber data.

Taylor microscale must depend linearly on time and inversely on the power exponent, n. In fact, for isotropic turbulence

$$\lambda^2 = -\frac{10}{n}\nu(t - t_o) \tag{34}$$

where t_o is some virtual origin. Thus an immediate test for a power law decay is to plot λ^2 versus t and fit a straight line as shown in Fig. 39.

Similar plots can be seen in all of the recent experiments and DNS; e.g., Antonia et al. [86], Antonia and Orlandi [87], Lavoie et al. [88], Burattini et al. [89], Hurst and Vassilicos [90], Lavoie et al. [91]. All identified substantial linear regions, clearly indicating a power law decay. Moreover the decay parameters were not the same, indicating a dependence on initial conditions.

One problem with the above methodology is that Eq. (26) has another parameter, the virtual origin in time, t_o, which can provide considerable freedom in choosing the optimal set. For example, Hurst and Vassilicos [90] note that:

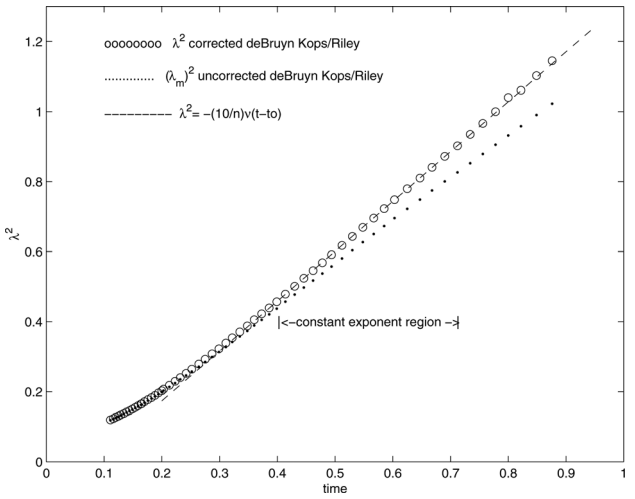

Fig. 39 Plot of λ^2 versus time for DNS of deBruyn Kops and Riley [83], from Wang and George [70]. Both original data and data corrected for missing lowest wavenumbers are shown.

> "…choosing the value of x_o (the virtual origin is $t_o = x_o/U$ *sic*)… gives values of $-n$ between 1.7 and 2.0 for the fractal cross grids and close to 2.3 for the classical grid. This x_o turns out to lie between −0.5 m and −1.2 m and is therefore well behind the grid."

Wang et al. [84] used a simultaneous regression on u^2, ε, and λ^2 with common parameters to minimize this problem. An even better approach to find the decay exponent which is possible with numerical data is to differentiate Eq. (26) to obtain

$$\frac{1}{\nu}\frac{d\lambda^2}{dt} = -\frac{10}{n} \tag{35}$$

From this the power, n, can be determined unambiguously with no ability to adjust a virtual origin. This was first proposed in George et al. [85] and used extensively by Wang and George [70] from which Figs. 40 and 41 were taken. Both illustrate nicely the path by which the DNS settles into the asymptotic power law state for the particular simulation, and also when it begins to depart from it as the scales of the computation grow too large for the computational domain. The flat regions in the graphs correspond to

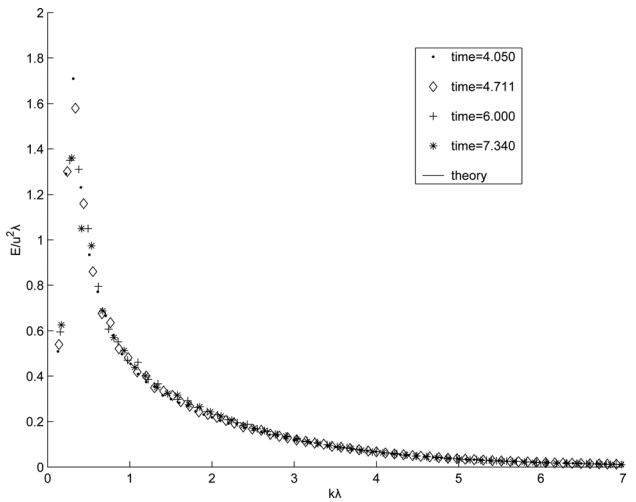

Fig. 38 Three-dimensional energy spectrum function, $E(k,t)$ plotted in Taylor variables using DNS data of Wray [82], from Wang and George [70]. Note that unscaled data varied by approximately a factor of 7 for the time segment shown. Also note the sparseness of low wavenumber data.

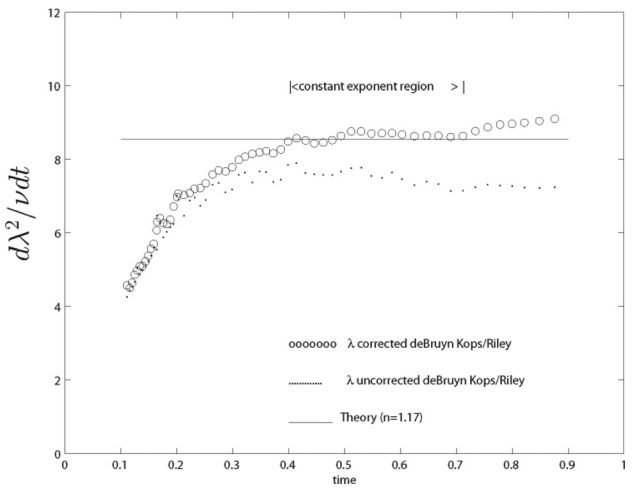

Fig. 40 Plot of $d\lambda^2/dt$ versus time for DNS of deBruyn Kops and Riley [83], from Wang and George [70]. The flat region corresponds to a region of power law decay. For the corrected data $n = -1.17$.

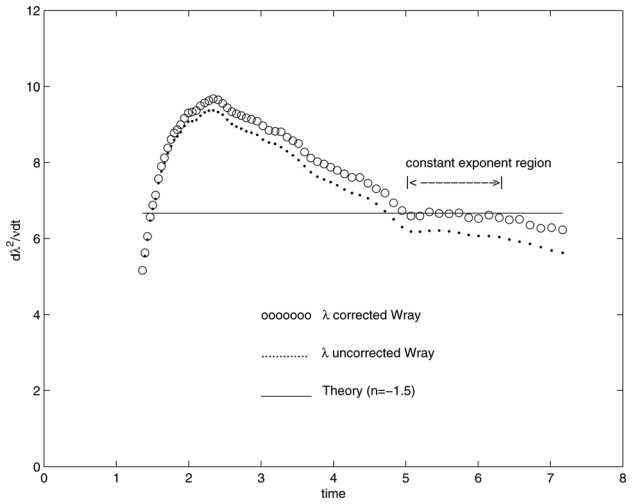

Fig. 41 Plot of $d\lambda^2/dt$ versus time for DNS of Wray [82], from Wang and George [70]. The flat region corresponds to a region of power law decay. For the corrected data, $n = -1.5$.

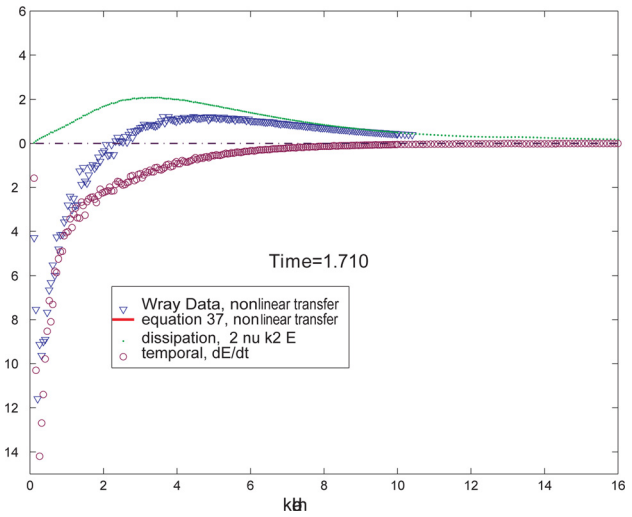

Fig. 43 Nonlinear transfer using DNS of Wray [82] and Eq. (36) with $n = -1.5$, from George and Wang [92]. Also shown are the dissipation spectrum and the spectrum of dE/dt.

$n = -1.17$ and $n = -1.5$ respectively, indicating a substantial difference arising from the initial conditions.

The interrelation of the energy decay exponent and the nonlinear spectral transfer can easily be obtained by substituting the various deduced results into Eq. (19) to obtain

$$G(\bar{k}) = -\frac{5}{n}[\bar{k}F' + F] - 10f + 2\bar{k}^2 F \tag{36}$$

where $G(\bar{k})$ is the nonlinear spectral transfer function and $F(\bar{k})$ is the energy spectrum, both normalized in Taylor variables. Note that there are no adjustable parameters. Figures 42 and 43 show excellent agreement between the computation and theory for the data of references [82] and [83] cited earlier; thus illustrating the internal consistency of both theory and data even though the spectra and decay rates are quite different.

Unfortunately, we do not yet have a theory as to what it is about the initial conditions that makes these decay rates different. But Burattini et al. [89] used a lattice Boltzmann simulation to carry out a systematic study of the effect of initial conditions, in particular to test the suggestion of George [11] that the decay exponent might tend toward $n = -1$ as the Reynolds number characterizing the initial conditions increased. They summarized their findings as follows:

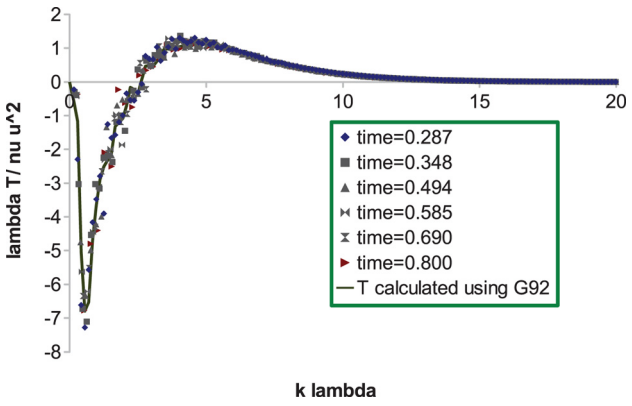

Fig. 42 Nonlinear transfer using DNS of deBruyn Kops and Riley [83] for all decay times and Eq. (36) with $n = -1.17$, from George and Wang [92]. Solid line shows computed spectral transfer.

> "The present data, together with other values available in the literature, suggest that $-n$ decreases towards 1, as $R_\lambda(0)$ (the initial value, *sic*) increases."

Clearly this idea merits further attention, but care must be taken to use only identical families of generators so as to not mix effects of Reynolds number with geometrical differences. Given the important role of the very largest scales probably even the ratio of tunnel (or computational box) size to generator size needs to be maintained as constant.

Do the Two-Point Statistics Really Collapse in Taylor Variables? One of the most surprising aspects of the equilibrium theory was that it in fact was able to collapse the pre-exisiting spectral data of both Comte-Bellot and Corrsin (Figs. 29 and 30) and Warhaft and Lumley (Fig. 33). Howeever, as noted above, the early DNS of decaying turbulence were problematical. Figures 37 and 38 show the spectra in Taylor variables for the two more recent DNS considered above for which the peak in the spectrum was well above the lowest wavenumber. Clearly the collapse is excellent, even on a linear-linear plot. Nonetheless, the lack of data at the lower wavenumbers complicates analysis.

Two of the many recent experimental evaluations of the spectral collapse postulated by the equilibrium similarity theory are shown in Figs. 44 and 45. Figure 44 shows the data from different

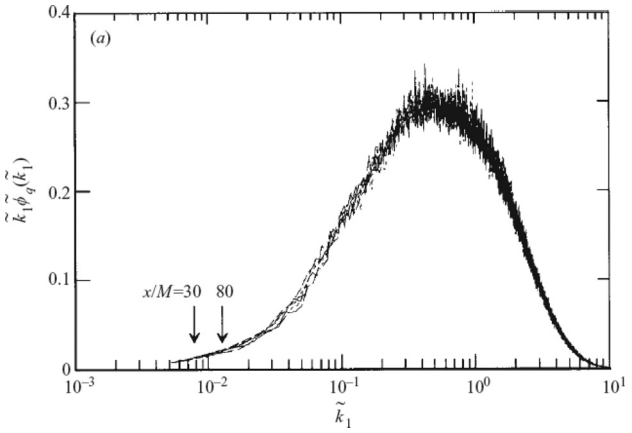

Fig. 44 Pre-multiplied longitudinal one-dimensional spectrum in Taylor variables, from Antonia et al. [86]

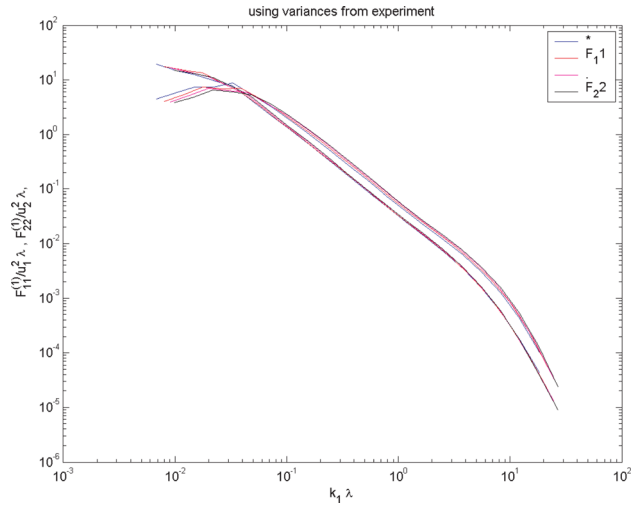

Fig. 45 Longitudinal and transverse one-dimensional velocity spectra normalized in Taylor variables for four downstream positions from active grid experiment of Kang et al. [93] as (provided by M. Wänström) (Longitudinal [- - -], Transverse [….]). Note the fact that the spectra do not flatten out for the lowest wavenumbers suggests strongly that the integral scales are not sufficiently well-resolved [6].

downstream positions of $k_1 F_{11}^{(1)}(k_1)$ (the so-called pre-multiplied spectrum) from the extensive experiments carried out using a classic square bar grid in the wind tunnel at the University of Newcastle by Antonia et al. [86]. Figure 45 depicts a re-plot by one of my former Ph.D. students, Maja Wänström, of the data for both the longitudinal spectra, $F_{11}^{(1)}(k_1)$, and the transverse spectra, $F_{22}^{(1)}(k_1)$, taken by Kang et al. [93] using an active grid in the Corrsin wind tunnel facility at the Johns Hopkins University. The Reynolds numbers achieved in this latter experiment are nearly an order of magnitude higher than that available with standard grids or DNS. Interestingly, the power law decay exponent for the Kang et al. [93] data was nearly the same as the Comte-Bellot and Corrsin data taken in the same wind tunnel decades earlier, even though the Reynolds number was an order of magnitude higher, the turbulence intensities much higher, and the grids very different. Clearly, the spectral collapse is excellent in all cases, strongly implying that this kind of turbulence can be characterized by the Taylor microscale at all scales of motion. Note that all these spectra collapsed to a unique curve for each set of initial conditions; thus confirming the postulated dependence on initial conditions.

Before leaving this section, we note that Antonia et al. [86] have considered the entire question of equilibrium similarity using the structure function equations. Structure functions are defined from moments of the difference in velocity between two points, e.g., the second order structure function defined by $\langle(\delta q)^2\rangle = \langle[u(x+r)-u(x)]^2\rangle$. The results are perfectly equivalent to the spectra, but since the structure functions consider separation instead of wavenumber, the plots emphasis different scales of motion. Figure 46 plots the longitudinal structure function normalized in Taylor variables from the wind tunnel experiment at the University of Newcastle corresponding to the spectral data shown above. Again the collapse is quite spectacular, emphasizing again the validity of the equilibrium similarity approach.

Antonia et al. [86] summarize their findings as follows:

> "The analysis and arguments presented… indicate that similarity of the transport equation for decaying homogeneous isotropic turbulence is possible when the characteristic velocity scale, $\langle q^2\rangle$ decays in power-law fashion, i.e., $\langle q^2\rangle \propto t^n$; and the characteristic length scale, which is identifiable with the Taylor microscale, grows as $\lambda \propto t^{1/2}$. The (local *sic*) turbulence Reynolds number, R_λ, can decay with t if the exponent $-n$ is smaller than 1. These results are in full accord with the results obtained by [11] by considering the spectral energy equation."

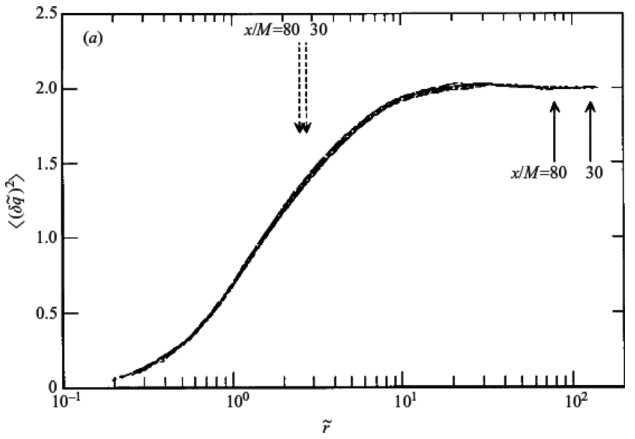

Fig. 46 Energy structure function in Taylor variables, from Antonia et al. [86]

Prediction before Measurement: Exponential Decay. One of the most interesting results in the past few years (at least from a theoretical point of view) has come from the work of Vassilicos and co-workers at Imperial College who used three different families of fractal grids (space-filling fractal-cross, fractal-I, and fractal-square) to examine decaying turbulence (e.g., Hurst [94], Hurst and Vassilicos [90], Seoud and Vassilicos [95]). The different grids clearly stamp their signature on the turbulence even far downstream, and the decay rate is most certainly not a single universal power law. The fractal-square family of grids even yields an exponential decay. Interestingly, the possibility of exponential decay was predicted in 1999 in a paper by Wang and George by considering equilibrium similarity solutions to Eq. (13) for which the length scale did not increase during decay. It was rejected for publication by two leading journals with the stated reason by the editors as: "…*since such turbulence has never been observed*," clearly an interesting criterion for advances in physics. Now such turbulence most certainly has been observed (as illustrated below), and happily the paper was published by a third journal as well [96], albeit a decade late.

Figure 47 from Hurst and Vassilicos [90] shows the particular family of grids (space-filling fractal square) which yields exponentially decaying turbulence. Curiously, other fractal designs produce power law decaying turbulence remarkably similar to

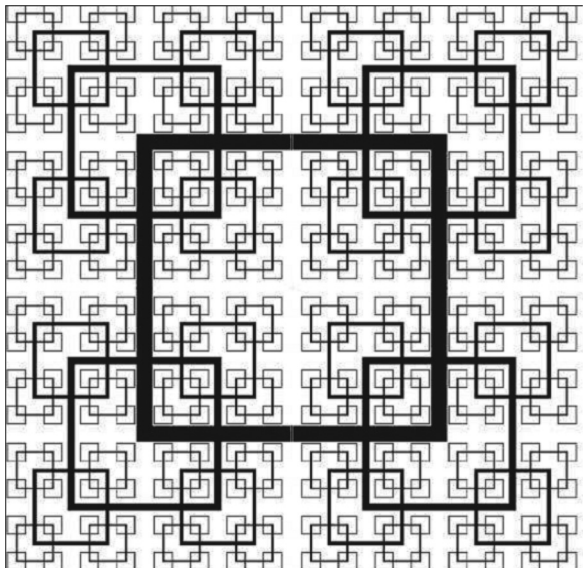

Fig. 47 Diagram of space-filling square fractal grid, from Fig. 33 of Hurst and Vassilicos [90]

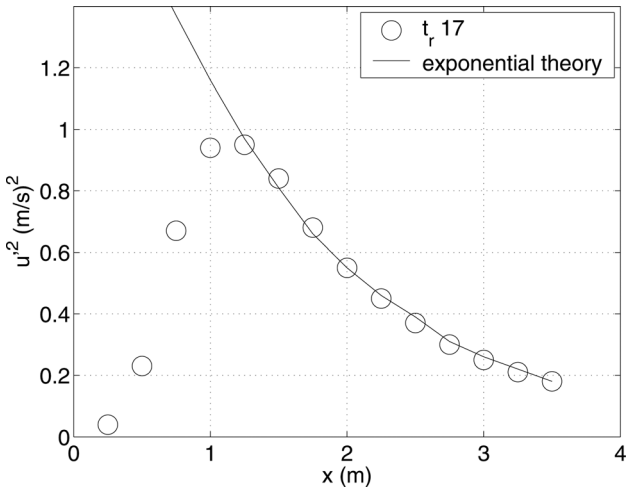

Fig. 48 Variation of turbulence intensity with downstream position for one space-filling fractal grid. Solid line shows exponential fit (from Hurst and Vassilicos [90]).

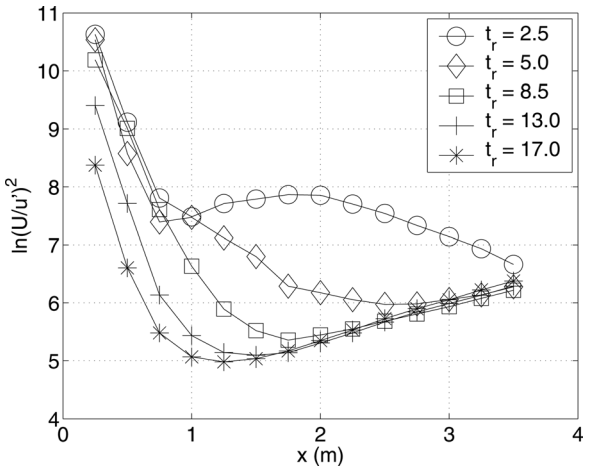

Fig. 49 Semi-log plot of variation of turbulence intensity for various space-filling fractal grids showing (with one exception) asymptotic exponential decay (linear region), from Hurst and Vassilicos [90]

classical grids (see Hurst and Vassilicos [90]). But for the family of grids shown in Fig. 48, the decay rate was very different.[7] Figure 49 shows a semi-log plot of the decay for the entire family of grids, along with an exponential fit to the data. All but one (the largest) eventually decay exponentially, and even it seems to be evolving in the same manner.

The Wang and George [96] theory predicted that the Taylor microscale should be constant during decay. Figure 50 makes it clear that for this exponentially decaying turbulence, it is. Moreover, the theory also predicted a constant ratio of integral scale to Taylor microscale, exactly as observed in Fig. 51. Finally, the theory predicted the spectral data should collapse when normalized in Taylor variables, v^2 and λ. Clearly, as shown in Fig. 52, they do.

Some Remaining Difficulties. For all of the nonstationary homogeneous flows considered herein, the equilibrium similarity theory makes predictions about the behavior of both the integral scale, L_{11} and the derivative skewness, $S_{\partial u/\partial x}$. In particular the equilibrium similarity theory argues that the physical integral scale, L_{11}, defined by Eq. (22) should be proportional to the Taylor microscale, λ. Also, the derivative skewness, $S_{\partial u/\partial x}$, should be inversely proportional to R_λ^{-1}. The constants of proportionality can depend only on the initial conditions. There has been considerable difficulty, however, consistently confirming these results with recent experiments and DNS, and both remain problematical. Therefore we consider each of these issues separately. From the perspective of this article, neither of these would be of concern were it not for the fact that only the equilibrium similarity theory (to this point at least) seems to be able to predict from first principles an asymptotic dependence on initial conditions. As such, the validity of theory and phenomenon would seem to be inextricably linked, at least until other theories appear. However, the fact that this theory also implies that the ratio $\varepsilon L_{11}/u^3$ is not constant during the time evolution of any of these nonstationary homogenous flows means that the Kolmogorov theory [77] cannot be universal and that has enormous implications.

[7]The fact that there were three families of fractal grids, only one of which behaved very differently was inexplicably (since the mistake was pointed out by a reviewer) ignored by Krogstad and Davidson [97] who used measurements behind grids from the fractal-cross family to challenge the surprising ICL findings from the fractal-square grids, and to argue for a universal decay law. A reanalysis of their data by Valente and Vassilicos [98] showed the K-D results to be both consistent with the earlier ICL results for such grids, and to exhibit a clear dependence on initial conditions. That JFM refused to publish their rebuttal illustrates the intransigence of some segments of the community to new ideas, and the extent some are willing to go suppress challenges to the classical thinking.

Integral scale, integral invariants, and domain size. Integral scales are routinely reported, but in fact are extraordinarily difficult to measure correctly. Moreover, they are very much influenced by the flow boundary conditions, and even the precise definition used to determine them experimentally varies from experiment to experiment. Both these problems can be related to a large degree to the breakdown of the 'assumed' homogeneity of experiments and simulations at the largest scales of motion. All experiments and DNS are performed inside finite boundaries. And it is the largest scales that contribute disproportionately to the integral scale. Figures 53 and 54 show the integrand of Eq. (22), $E(k,t)/k$, normalized in Taylor variables for both DNS data sets considered earlier. Clearly neither provides enough resolution at low values of k to make a reasonable integral scale determination. Figure 55 from Wang and George [70] shows the ratio of the integral scale to Taylor microscale from the DNS data of deBruyn Kops and Riley [83], both before and after attempting to compensate for the missing lowest wavenumbers from the finite 'box size' of the simulation. A simple spectral model showed that the wavenumber of the spectral peak of the simulation needed to be about 10 times larger than that of the lowest wavenumber of the simulation to correctly estimate the integral scale. This criterion is even more severe if its time variation is of interest, since the

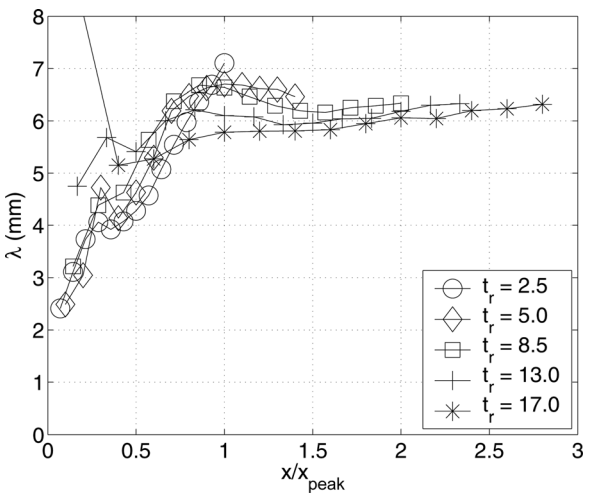

Fig. 50 Downstream variation of Taylor microscale, λ, for different upstream conditions (from Hurst and Vassilicos [90].)

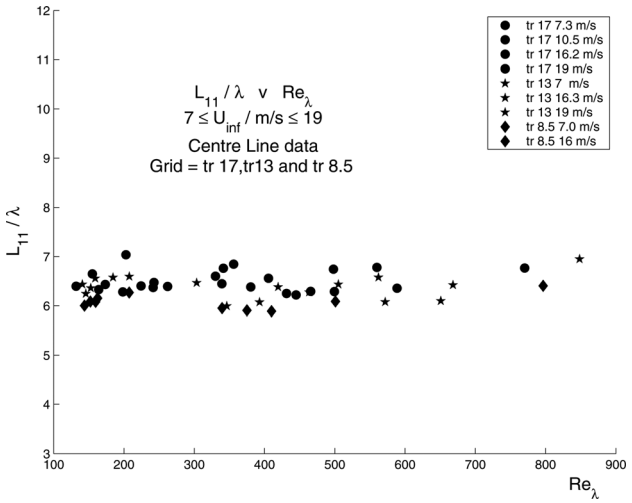

Fig. 51 Ratio of integral scale to Taylor microscale for different upstream conditions (from Seoud and Vassilicos [95])

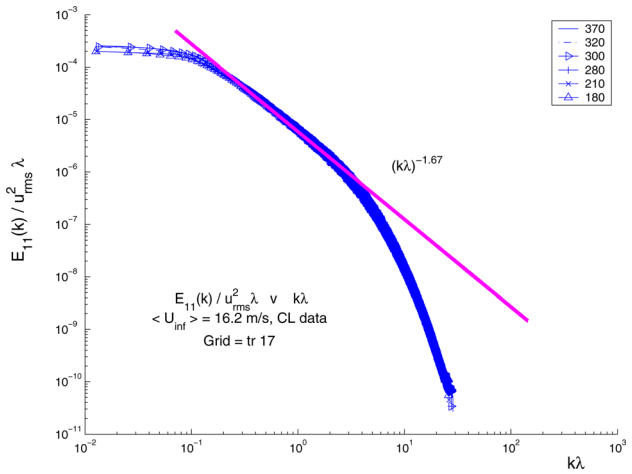

Fig. 52 One-dimensional spectra showing collapse during decay with u^2 and λ. Legend denotes downstream position (from Seoud and Vassilicos [95]).

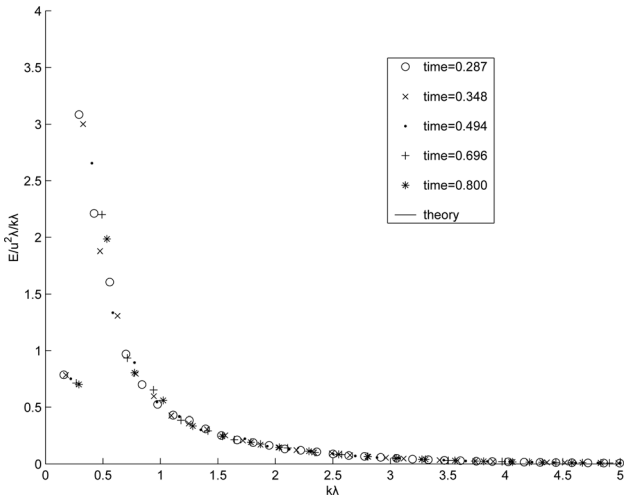

Fig. 53 Integrand of integral scale spectral integral, $E(k,t)/k$ plotted in Taylor variables using DNS data of deBruyn Kops and Riley [83], from Wang and George [70]. Note the sparseness of low wavenumber data.

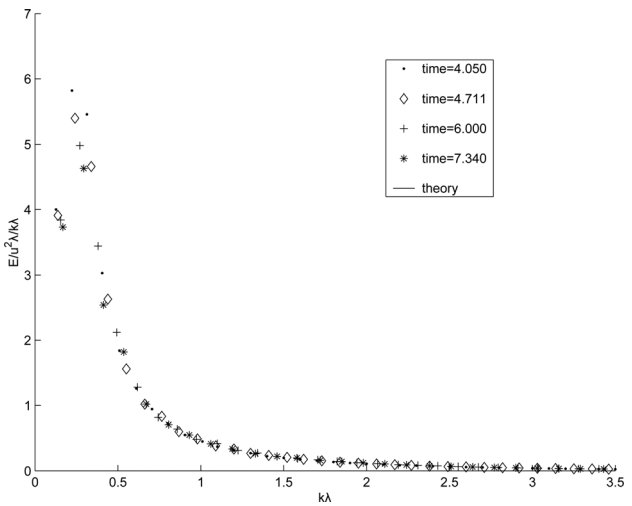

Fig. 54 Integrand of spectral integral, $E(k,t)/k$ plotted in Taylor variables using DNS data of Wray [82], from Wang and George [70]. Note the sparseness of low wavenumber data.

relative errors in its determination are themselves time-dependent. Clearly compensating for the missing scales is far less satisfactory than in simulating them correctly to begin with, since this is only *kinematic* correction. The most important question is: How much greater than the integral scale must the extent of the flow be to insure that the simulation or experiment is in fact *dynamically* representative of a mathematically homogeneous flow which by definition must be of infinite extent? Until this question is resolved, the behavior of the integral scale must be regarded as unresolved, but it is likely related to the question of integral invariants discussed in the following paragraph.

That there might be a relation between integral invariants and dynamics was first raised by Loitsianskii [99], at least for the decay of homogeneous turbulence. Reference [67] provides an extensive review of the resulting debate over many years; Refs. [100,101] provide more recent contributions. The m-th order integral invariant, $I_m(t)$, is defined by

$$I_m(t) = \int_0^\infty r^m B_{1,1}(r,0,0,t)dr \tag{37}$$

where $B_{1,1}(r,t) = \langle u_1(x,y,z,t)u_1(x+r,y,z,t)\rangle$ and is the inverse Fourier transform of the one-dimensional velocity spectrum, $F_{1,1}^{(1)}(k_1,t)$. For example, $m=0$ corresponds to the integral scale (discussed in the preceding paragraph) times $\langle u_1^2\rangle$, $m=2$ corresponds to the so-called Saffman integral and $m=4$ to the Loitsianskii integral (see Ref. [67]). Note that there are variations on these integrals using $B_{i,i}(\vec{r})$, the trace of the two-point velocity correlation, instead of the streamwise correlation, $B_{1,1}(r)$. By assuming a simple exponential behavior, $B_{1,1}(r,t) = u^2 e^{-|r|/L_{11}}$, it is easy to show that many integral scales of data are necessary to estimate these to a high accuracy, *even if the flow is truly representative of a homogenous flow*. But most importantly, if one is interested in the *time variation of these quantities*, then it is the time variation of the truncation error that is of primary concern, so even much more restrictive criteria must be applied (i.e., many many integral scales). As a consequence, these issues remain very much in doubt, and are likely to remain so for some time. Unfortunately, it is precisely this missing information that tells us how boundaries affect the turbulence everywhere, so they most likely have implications for numerical simulations and experiments of all types, not just homogeneous turbulence.

Derivative skewness and small scale resolution. The same concerns apply to attempts to measurement the derviative

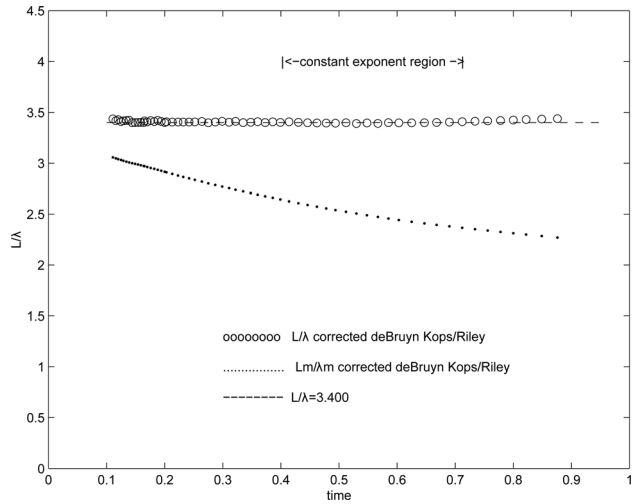

Fig. 55 Plot of L_{11}/λ versus time for DNS of deBruyn Kops and Riley [83], from Wang and George [70]

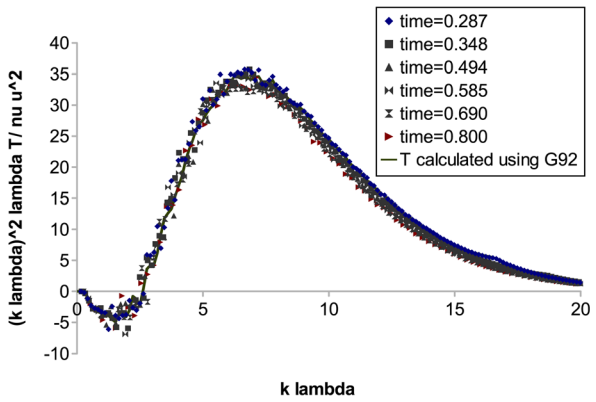

Fig. 56 Second moment of three-dimensional spectral transfer, $k^2T(k,t)$ plotted in Taylor variables using DNS data of deBruyn Kops and Riley [83]

skewness. The derivative skewness may seem to most engineers to be one of those strange quantities that only true turbulence experts worry about. But it is easy to show that it lies at the heart of one of the most unresolved problems in turbulence modeling, namely how to model the dissipation equation. A spectral dissipation equation for homogeneous turbulence can readily be obtained from Eq. (13) by multiplying it by $2\nu k^2$; i.e.,

$$\frac{\partial}{\partial t}\left[2\nu k^2 E\right] = 2\nu k^2 T - 4\nu^2 k^4 E \tag{38}$$

Integrating this equation over all wavenumbers leads immediately to the homogeneous dissipation rate equation; i.e.,

$$\frac{d\varepsilon}{dt} = P_\varepsilon - D_\varepsilon \tag{39}$$

where P_ε represents the 'production' of dissipation and D_ε represent the 'dissipation' of dissipation. If we leave out the factor of 2ν in Eq. (38), we have instead the balance equation for the mean square vorticity. This is because for a homogeneous flow $2\langle s_{ij}s_{ij}\rangle = \langle \omega_i\omega_i\rangle$ where s_{ij} is the fluctuating strain-rate tensor and ω is the fluctuating vorticity. In this latter equation, the 'production' term can be readily interpreted as the amplification of new fluctuating vorticity from old by the stretching and turning of vortex lines by the turbulence itself. Regardless of which form we use, it is clear that the production of both dissipation and fluctuating vorticity is reflected in the integral of k^2T, the second spectral moment of the nonlinear spectral transfer term. For isotropic turbulence this integral is directly related to the velocity derivative skewness, $S_{\partial u_1/\partial x_1}$, by

$$S_{\partial u_1/\partial x_1} = \frac{\langle[\partial u_1/\partial x_1]^3\rangle}{\langle[\partial u_1/\partial x_1]^2\rangle^{3/2}} = -\frac{3\sqrt{30}}{14}\frac{\int_0^\infty k^2 T(k,t)dk}{\left[\int_0^\infty k^2 E(k,t)dk\right]^{3/2}} \tag{40}$$

The velocity derivative skewness is therefore a direct measure of the role of the nonlinear spectral transfer—in fact our lowest order measure, since the integral of $T(k,t)$ itself is identically zero. Thus, it has considerable theoretical significance, especially since different theories of turbulence predict different behaviors for it. For example, in the classical Kolmogorov-based theories it is predicted to be a universal constant for decaying turbulence (typically about 0.5), but in the intermittency-based models to increase with Reynolds number [67,102]. In the G92-type similarity approach outlined above, the product $S_{\partial u_1/\partial x_1}R_\lambda$ is predicted to be constant *during decay*, but to increase with the ratio of integral scale to Taylor microscale which is itself constant during decay but depends (in some unknown way) on the Reynolds number of the initial conditions (e.g., the grid Reynolds number in a wind tunnel). These differences among theories would seem to provide direct tests of the validity of any theory.

Unfortunately, $S_{\partial u_1/\partial x_1}$ has also proven to be extraordinarily difficult to simulate or measure, and accurate determination in any flow remains a significant challenge to the next generation DNS and experimental communities. Figure 56 shows the second spectral moment in Taylor variables of the nonlinear transfer data of Ref. [83] presented in Fig. 42. The first term on the right-hand-side is always negative (in decaying turbulence), so it is the emergence of the last term on the right-hand-side with increasing wavenumber that accomplishes the necessary sign change. Obviously failure to resolve high enough wavenumbers (or small enough scales) to accurately determine the last integral will very much affect the results. The near collapse in Taylor variables is consistent with the equilibrium similarity results and $S_{\partial u_1/\partial x_1}R_\lambda = const$; however, in contradiction, integration over all wavenumbers shows $S_{\partial u_1/\partial x_1} \approx const$. The differences can be shown to be entirely due to contributions to the integral from wavenumbers larger than $1/\eta_{Kol}$. This is problematical since most numerical simulations are performed to resolve to approximately $k\eta_{Kol} \approx 1$, where $\eta_{Kol} = (\nu^2/\varepsilon)^{3/4}$) is the so-called 'Kolmogorov microscale.' This is sometimes erroneously referred to as the 'smallest scale of the turbulence.' It is, of course, not the smallest scale of the turbulence! The turbulence scales diminish with diminishing energy all the way to infinitesimal (or in practice until the continuum limit). In fact, herein is another misunderstanding that is widespread in the turbulence field, especially among those focused on applications. It is generally believed that the Kolmogorov microscale is the smallest dynamically significant length 'scale' which can be defined from the parameters in the spectral equations. It is not. There are many smaller length scales which can be defined from the higher order spectral equation and their integrals. For example using ε_ε, the dissipation of the dissipation (familiar to all turbulence modelers) defined from the integral of the last term in Eq. (38) as

$$\varepsilon_\varepsilon = 4\nu^2 \int_{-\infty}^{\infty} k^4 E(k)dk \tag{41}$$

a dissipation of dissipation length scale can be defined as $\eta_{\varepsilon_\varepsilon} = (\nu^4/\varepsilon_\varepsilon)^{1/6}$. This process of definition can be continued indefinitely using the dissipation of the dissipation of the dissipation, etc. Clearly $\eta_{\varepsilon_\varepsilon}$ plays the analogous role in the fluctuations

dissipating the dissipation that the Kolmogovor microscale, η_{Kol}, itself plays in the energy dissipation. But what is that? Why do we care about the Kolmogorov microscale?

The answer is this: η_{Kol} is of practical interest because it is the wavenumber below which about 99% of the dissipation occurs; i.e., $2\nu \int_0^{1/\eta_{Kol}} k^2 E dk \approx 0.99\varepsilon$. In other words, the contributions to the dissipation integral of Eq. (20) are essentially negligible above $k\eta_{Kol} = 1$ or slightly smaller. So if we are only interested in the overall energy balance, this is enough resolution. Unfortunately, this is not true for the last integral of Eq. (38), since its integrand depends on $k^4 E$, which can have significant contributions above $k\eta_{Kol} = 1$ (in fact to approximately $k\eta_{\varepsilon_\varepsilon} = 1$), and this in turn can make estimates of the integral of $k^2 T$ and the derivative skewness very much in doubt. Similar considerations must apply to attempts to measure as well.

There is another serious consequence for DNS of this finite resolution as well (v. Ref. [103].) which is especially important in a statistically nonstationary turbulence (like decaying turbulence), which can make an entire simulation into doubt. If the integral of $k^6 E$ is not resolved, then this affects the balance equation for the dissipation of the dissipation which depends on $k^4 E$, and that in turn affects $k^2 E$ through Eq. (38), and finally quite directly, the energy. If all the scales are growing with time, then things improve with time. More subtle but of equal concern is: where does the energy that should have gone to even higher (or lower) wavenumbers actually go? Clearly because the nonlinear interactions of the turbulence in a homogeneous flow move energy among triads of wavenumbers, the energy either piles up at the extremes or is redirected to wavenumbers where it should not be. When this happens, the simulation can no longer be considered an approximation to a homogenous turbulence, but rather is a periodic flow in a box. Two clues that this is happening in DNS for example are that the three-dimensional spectrum function, $E(k,t)$ starts filling in at the lowest wavenumber *and* at the very highest wavenumbers. This very much affects both the integral and spectral moments, rendering both unreliable.

Wind tunnel experiments at least avoid part of this problem, since the flow itself produces the finest scales possible, at least eventually. Measuring them accurately can be an almost impossible challenge though, particularly because of the problem of having probes sufficiently small to measure fourth spectral moments to sufficient accuracy and to be able to accurately determine how they change in time. Also, the errors induced by using Taylor's hypothesis to estimate either dissipation or derivative skewness can introduce a significant apparent but unreal time variation all by itself [104,105]. This arises due to the leakage down the spectrum caused by the fluctuating convection velocity introduced by the finite (and varying) turbulence intensity [106]. Figures 57 and 58 from Burattini et al. [107] illustrate the problem nicely. They show respectively how $S_{\partial u_1/\partial x_1}$ and its product with R_λ vary downstream of a grid. Depending on what part of the flow is considered and whether data are corrected or not, almost any hypothesis can be supported. A new generation of careful experiments in very large facilities is clearly needed to sort this out.

Kolmogorov turbulence: 'local' equilibrium or not? Finally, although tangential to the issue of asymptotic sensitivity to initial conditions, the universality and applicability of Kolmogorov thinking to at least the nonstationary homogeneous flows considered herein has been challenged both theoretically and experimentally (see Refs. [11,95,108]. In particular, the nonstationary results appear to be inconsistent with at least some ideas long accepted as fact: among them, the interpretation of u^3/ε as proportional the physical length scale, L_{11}[8] and the universal scaling of the dissipative motions (note that the discrepancies arise only for flows whose statistical quantities vary in time, or at least flows which closely approximate them). At the very core of Kolmogorov's

[8]So predominant is this view that many actually call u^3/ε the integral scale, even though a correct application of K41 thinking suggests that it must at least be Reynolds number dependent for a fixed geometry (see Ref. [109]).

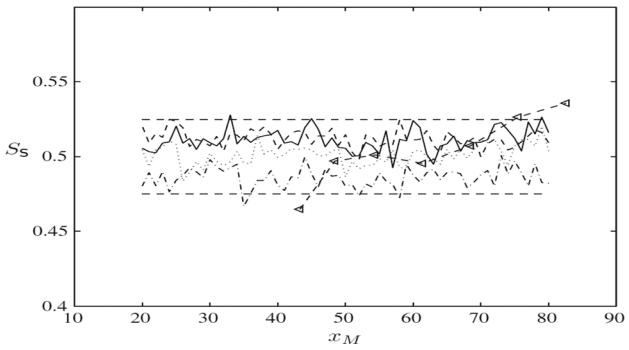

Fig. 57 Burattini et al. [107] measurements of derivative skewness in decaying grid turbulence (corrected and uncorrected)

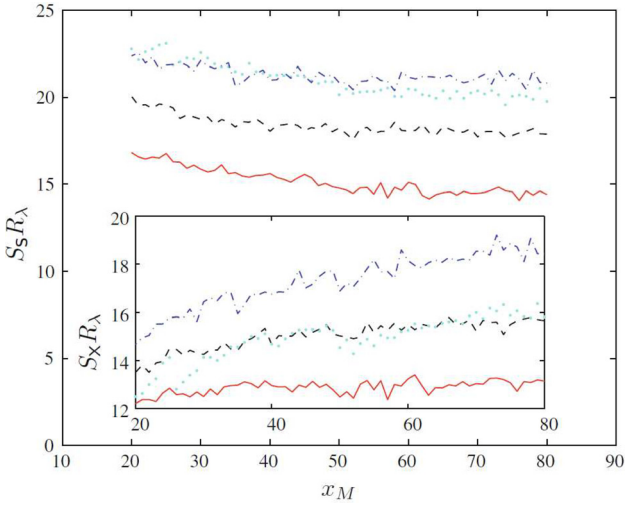

Fig. 58 Burattini et al. [107] measurements of derivative skewness times R_λ in decaying grid turbulence (corrected and uncorrected)

arguments was the assumption of *local equilibrium*, meaning that the smallest scales of motion (highest wavenumbers in Batchelor's interpretation [66]) could be considered in statistical equilibrium. This is usually justified by time scale arguments using the fact that the time scales of the smallest eddies (or highest wavenumbers) are very small compared to those at the energetic scales, and this difference increases with increasing Reynolds number. From this it is argued that in Eq. (13), for example, that $\partial E/\partial t \ll T$ or $2\nu k^2 E$ for the high wavenumbers, and therefore can be neglected relative to them. Thus the *local equilibrium* of the smallest scales is postulated (or highest wavenumbers). If the theory and experiments reviewed earlier are correct, then this assumption is not valid for these flows, since all scales (or wavenumbers) evolve together. It is easy to see the flaw in the time scale argument, since the time scale argument makes the implicit assumption that the scaling of changes in E are the same at all wavenumbers. Clearly they are not.

There have been other clues as well that nonequilibrium turbulence may march to a different drummer than the commonly assumed Kolmogorov ideas of local equilibrium would imply. Yeung et al. [68] summarized their extensive numerical experiments on distant triadic interaction in homogeneous turbulence as follows:

> The results indicate that non-equilibrium non-stationary turbulence is particularly sensitive to long-range interactions and deviations from local isotropy.

In other words, with reference to Fig. 28, it is the wavenumbers which are *not* of nearly equal length, which are important. Moreover they further state:

> This work indicates that Fourier modes, and their corresponding scales of motion, are dynamically coupled over large separation in scale, the strength of the coupling increasing with the relative energies of the large- and small-scale modes. Within the individual triads, then, the strongest couplings tend to be between the large energy-containing scales and the dissipative scales with local Reynolds number of order one or greater. Because an element of small-scale evolution is coupled to the structure and evolution of the large scales with the distant triadic group, if the large scales have a statistically preferred direction, the energy transfer within the distant group of triadic interactions also has a preferred direction. This directional dependence persists in ensemble averages of statistically similar flows. The distant group, then, is in principle at variance with the Kolmogorov hypothesis of statistical large-small scale independence in the asymptotic limit (Yeung et al. [68]).

The examples cited herein of nonstationary turbulence would seem to behaving in a manner consistent with these observations.

Summary and Conclusions

It is clear from all the flows considered herein that initial conditions play an important role in the development of turbulent shear flows, and even in nonstationary homogeneous turbulent flows. We have considered only flows for which there is a corresponding *equilibrium similarity solution* consistent with experimental observations. There do exist, however, other classes of flows where recent observations have shown the influence of initial/upstream conditions, but which for the sake of compactness have not been covered in the above discussion. Prominent examples include the shear layers of Slessor et al. [110] and flows with buoyancy effects and density variations; e.g., the Rayleigh-Taylor flows of Ristorcelli and Clark [111], Ramaprabhu et al. [112], Mueschke et al. [113],Youngs [114], and even multiphase flows, e.g., Arndt and Wosnik [115]. In addition, it has become quite respectable to consider that turbulent boundary layers might grow at rates determined by the initial conditions; e.g., Cal et al. [116], Castillo and George [19,20].

Thus, while there might have been reasons to doubt the role of initial conditions 20 years ago, or even to question the experiments or a new theory, the careful studies of the past two decades have made it clear that theory and experiment are in agreement: initial (and/or upstream) conditions do matter. In some flows they do not matter very much; in other flows, they matter a great deal. Regardless of the degree of importance, they are problematical for engineers because no single point turbulence model can account for them, since the initial conditions are buried in the model constants. Thus there can be no universal single point model for turbulence, not that anyone really recently believed there could be. Structure-based models can perhaps account for the observed differences, but only if we can establish which properties of the initial (or upstream) flow need to be accounted for. By contrast, LES seems to retain all of the essential information, or at the very least can reflect differences in how the flow is started. But again, the question remains: what information should be provided initially?

Unfortunately, our theoretical understanding of how initial conditions can persist has progressed less rapidly than our recognition that they do. It is, however, of rapidly increasing interest. See for example the papers from the 'Symposium on initial conditions in turbulence' organized by Fernando Grinstein at the 2003 AIAA meeting in Reno, NV and published in the Mar. 2004 issue of the AIAA Journal. However, the future of LES is really bleak if we have to run a DNS to begin every computation, just to make sure we get the right starting details. The recent success of the LEA/Poitier group using POD to provide LES initial conditions is at least a step in the right direction of simplifying the requirements (vis. Drualt et al. [117]). Another interesting approach is by David Youngs [114] of AWE in the UK who has used LES in Rayleigh-Taylor flows to explore a possible coupling between initial conditions and boundary conditions.

Regardless of the issues above, it seems that a properly constructed equilibrium similarity theory (when such solutions exist) is both consistent with the observations and can even be said to "predict" them. Moreover, theory and experiments together imply that the usually assumed universality of Kolmogorov thinking does not apply to at least these nonstationary flows, since they do not satisfy his local equilibrium hypothesis. What we do not know is whether these *equilibrium similarity* flows are unique in their ability to remember how they were generated, or whether this is a general feature of most turbulent flows. It is quite important to know this. If the similarity flows are indeed 'special', they would not be representative of flows of engineering interest. So we should not be using them to create (or calibrate) models for turbulence. On the other hand, if these simple flows are representative, then they could provide wonderful platforms for investigating how initial (or upstream) conditions are propagated, and for testing models which retain the right dependencies. And that is, of course, what we would really like to know, especially if we are interested in trying to control or tailor flows by how we start them: this would be real turbulence control.

Acknowledgment

The idea for this paper grew out of an invitation to speak at the Ankara International Aerospace Conference, Ankara, Turkey, Sept. 10–12, 2007 while I was Professor of Turbulence at Chalmers Technical University. I am especially grateful to Ismail Tuncer of at the METU (Middle East Technical U.) for providing that opportunity. I would also like to pay special tribute to my former students from several institutions, Ph.D., Masters, and Post-docs, who have contributed much to the development of the ideas presented herein, often by simply participating in classroom and coffee room discussions. Directly involved at various times in the research were Dan Ewing, Joe Citriniti, Luciano Castillo, David Zielke, Asad Sardar, Martin Wosnik, Stephan Gamard, Daehan Jung, Honglu Wong, James Sonnenmeier, Peter Johansson, Maja Wänström and Abolfazl (Farzad) Shiri; and as well my former colleagues at SUNY/Buffalo and Chalmers, Dale Taulbee and T. Gunnar Johansson respectively. I would also like to acknowledge the initial interest and support of Mike Gibson (Imperial College, now retired); and also Mike Rogers and Bob Moser (both then at NASA Ames), beginning in the mid-90's, both of whom helped rescue the turbulent shear flow results from oblivion. And I am personally grateful for the many recent contributions of Bob Antonia and his co-workers at the U. of Newcastle and elsewhere and Christos Vassilicos and his co-workers at Imperial College; they have added much to our understanding of these most interesting phenomena. Arkady Tsinober (Tel Aviv), Christos Vassilicos (Imperial) and Ian Castro (Southhampton) also provided helpful comments on the manuscript. A short visit to the University of Wyoming in 2008 was critical to the first version of this paper. This work was completed while the author was a Visiting Professor at Ecole Centrale de Lille, University of Lille Nord de France and as a Marie Curie Fellow at the Department of Aeronautics of Imperial College of London. The support of these institutions and the European Union Marie Curie Program is greatly appreciated.

Nomenclature

A = constant defined by Eq. (25)
B = constant defined by Eq. (26)
$B_{1,1} = \langle u_1(x,y,z,t)u_1(x+r,y,z,t)\rangle$, (m)
$B_{i,i} = \langle u_i(x,y,z,t)u_i(x+r,y,z,t)\rangle$, (m)
C = constant defined by Eq. (27)
D = jet diameter, (m)
D_* = effective jet diameter, defined by Eq. (8), (m)
D_o = drag per unit length per unit mass, (m^3/s^2)
DNS = direct numerical simulation
E = three-dimensional energy spectrum function of wavenumber k, (m^2/s^3)

$E_{11} = 2F_{11}^{(1)}$, (m^2/s^3)
E_s = energy scaling function defined by Eq. (22), (m^3/s^2)
F = dimensionless spectrum defined by Eq. (22)
f = dimensionless velocity profile, generally function of η and initial conditions
F_o = rate at which buoyancy is added at axisymmetric source, (m^3/s^2)
$F_{11}^{(1)}$ = one-dimensional wavenumber spectrum of streamwise velocity, (m^3/s^2)
$F_{22}^{(1)}$ = one-dimensional wavenumber spectrum of cross-stream velocity, (m^3/s^2)
$F_{\theta\theta}^{(1)}$ = spectrum of temperature fluctuations, $((\deg \mathrm{K})^2 m)$
G = dimensionless energy transfer function defined by Eq. (23)
g = dimensionless Reynolds stress profile, generally function of η and initial conditions
G_o = rate at which angular momentum per unit mass is added to jet, (m^5/s^2)
$\vec{k}$ = wavenumber, (m^{-1})
K = $= dU/dy$, mean shear rate in homogeneous shear flow, (s^{-1})
k = magnitude of wavenumber, $k = |\vec{k}|$, (m^{-1})
$\bar{k}$ = wavenumber, k, nondimensionalized by L
$\tilde{k}$ = wavenumber nondimensionalized by λ
k_1 = streamwise component of wavenumber $\vec{k}$, (m^{-1})
k_1 = nondimensional wavenumber, $= k_1\lambda$
L = similarity length scale to be determined by analysis, (m)
L_o = plane wake 'width' defined in Ref. [4] as $2U_oL_o = U_\infty\theta$, (m)
L_M = buoyancy (or 'Morton') length scale defined by Eq. (10), (m)
L_s = swirl length scale defined by Eq. (11), (m)
L_{11} = integral length scale defined by Eq. (29), (m)
M = mesh size for wind tunnel grid, (m)
M_o = rate at which momentum per unit mass is added at axisymmetric source, (m^4/s^2)
m_o = rate at which mass per unit mass is added at source, (m^3/s^2)
n = exponent for power law decay of turbulence energy in decaying turbulence
P_ε = rate of production of turbulence dissipation by turbulence itself, (m^2/s^4)
R_λ = $= u\lambda/\nu$, Reynolds number based on turbulence intensity and Taylor microscale
r = radial r, (m)
q = kinetic energy scale, defined by $q^2 = u_iu_i = 3v^2$, (m/s)
$r_{1/2}$ = half-width of pulsed jet, distance from centerline where $U = U_c/2$, (m)
$\tilde{r}$ = $= r/\lambda$
R_s = x-dependent Reynolds stress scale to be determined by equilibrium similarity analysis, (m/s)
S = swirl number defined as $S = 2G_o/M_oD$
S_* = effective swirl number defined as $S_* = 2G_o/M_oD_*$
$S_{\partial u_1/\partial x_1}$ = derivative skewness, $[\langle \partial u/\partial x]^3\rangle/\langle[\partial u/\partial x]^2\rangle^{3/2}$
T = nonlinear spectral transfer from triadic interactions, (m^3/s^3)
t = Time, (s)
T_s = scale function for spectral energy transfer defined by Eq. (23) (m^3/s^3)
u_i = fluctuating velocity vector, (m/s)
u = $\sqrt{\langle u_iu_i\rangle/3}$, velocity fluctuation, (m/s)
u_1 = 1-component of fluctuating velocity, (m/s)
u_2 = 2-component of fluctuating velcocity, (m/s)
u' = RMS fluctuating velocity, (m/s)
v = cross-stream (plane flows) or radial (axisymmetric) flows fluctuating velocity, (m/s)
U = streamwise velocity, generally function of position, (m/s)
U_c = centerline mean velocity, (m/s)
U_j = jet exit velocity for top-hat jet, (m/s)
U_o = centerline mean velocity deficit for wakes, $U_\infty - U_{cl}$; but mean convection velocity for homogeneous shear flow turbulence, (m/s)
U_s = x-dependent velocity scale to be determined by equilibrium analysis, (m/s)
U_* = effective jet velocity, defined by Eq. (9), (m/s)
U_∞ = free stream value of streamwise velocity, (m/s)
V = cross-stream (plane) or radial (axisymmetric) mean velocity, (m/s)
v = cross-stream (plane) or radial (axisymmetric) fluctuating velocity, (m/s)
W = azimuthal component of mean velocity, (m/s)
x = streamwise coordinate, (m)
x_M = x/M, streamwise coordinate normalized by grid mesh
x_o = virtual origin for streamwise coordinate, (m)
x_{peak} = streamwise coordinate at which energy peaks downstream of fractal grid, (m)
$\bar{x}$ = dimensionless streamwise wake coordinate measured from virtual origin, $(x - x_o)/2\theta$, (m)
y = cross-stream coordinate in plane flows, (m)
δ = x-dependent length scale, determined by equilibrium similarity analysis, (m)
$\langle(\delta q)^2\rangle$ = velocity structure function, $= \langle[u(x + r, y, z, t) - u(x, y, z, t)]^2\rangle$, (m^2/s^2)
$\langle(\tilde{\delta q})^2\rangle$ = structure function nondimensionalized by $\langle u_1^2\rangle$
δ_* = axisymmetric wake 'width' defined in Ref. [31] as $U_o^2\delta_* = U_\infty^2\theta$, (m)
$\delta_{1/2}$ = jet half-width, distance from centerline where $U = U_c/2$, (m)
ε = local rate of dissipation of turbulence kinetic energy per unit mass, (m^2/s^3)
ε_ε = local rate of dissipation of dissipation per unit mass, (m^2/s^4)
η = dimensionless similarity coordinate, $= y/\delta(x)$ or $r/\delta(x)$
η_{Kol} = Kolmogorov microscale, $= (\nu^3/\varepsilon)^{1/4}$, (m)
$\tilde{\phi}_{ij}$ = nondimensional 1-dim. velocity spectra, same as $F_{i,j}^{(1)}(k_1, t)/\langle u_1^2\rangle\lambda$, (m^3/s^2)
λ = Taylor microscale, defined by Eq. (30), (m)
λ_θ = Taylor microscale of temperature fluctuations, $= \langle\theta^2\rangle/\langle[\partial\theta/\partial x_1]^2\rangle$, (m)
ν = kinematic viscosity, (m^2/s)
ρ = fluid density, (kg/m^3)
θ = momentum thickness, defined for plane wake by Eq. (2), (m)
υ = turbulence velocity scale defined by Eq. (18), (m/s)
$*$ = argument representing possible dependence on initial or upstream conditions, (m/s)
$'$ = denotes differentiation by η; i.e., $d/d\eta$, (m^{-1})
$\langle\ \rangle$ = indicates ensemble average

References

[1] Hussain, A., 1983, "Coherent Structures-Reality and Myth," *Phys. Fluids*, **26**, pp. 2816–2850.
[2] Bevilaqua, P. M., and Lykoudis, P., 1978, "Turbulence Memory in Self-Preserving Wakes," J. Fluid Mech., **89**, pp. 589–606.
[3] Sreenivasan, K. R., and Narasimha, R., 1982, "Equilibrium Parameters for Two-Dimensional Turbulent Wakes," Trans. ASME J. Fluids Eng., **104**, pp. 167–169.
[4] Wygnanski, I., Champagne, F., and Marasli, B., 1986, "On the Large-Scale Structures in Two-Dimensional Small Deficit, Turbulent Wakes," J. Fluid Mech., **168**, pp. 31–71.
[5] Townsend, A., 1976, *Shear Flow Turbulence*, Cambridge University Press, Cambridge, UK.
[6] Tennekes, H., and Lumley, J., 1972, *A First Course in Turbulence*, MIT Press, Cambridge, MA.
[7] George, W., 1989, "The Self-Preservation of Turbulent Flows and its Relation to Initial Conditions and Coherent Structures," *Advances in Turbulence*, W. George and R. Arndt, eds., Hemisphere, New York, pp. 1–41.
[8] Taulbee, D., 1989, "Reynolds Stress Models Applied to Turbulent Jets," *Advances in Turbulence*, W. George and R. Arndt, eds., Hemisphere, New York, pp. 29–73.

[9] George,W., and Arndt, R., 1989, *Advances in Turbulence*, Hemisphere, New York.
[10] George, W. K., 1995, "Some New Ideas for Similarity of Turbulent Shear Flows," *Proceedings of the Symposium on Turbulence, Heat and Mass Transfer*, Lisbon, Portugal, Aug. 9–12 1994, Hanjalic and Pereira, eds., Begell House, pp. 24–49.
[11] George, W. K., 1992, "The Decay of Homogeneous Isotropic Turbulence," *Phys. Fluids A*, **4**(7), pp. 1492–1509.
[12] George, W., 1990, "Self-Preservation of Temperature Fluctuations in Isotropic Turbulence," *Studies in Turbulence*, C. G. S. T. B. Gatski, S. Sarkar, eds., Springer Verlag, Berlin, pp. 514–427.
[13] George, W. K., and Gibson, M. M., 1992, "The Self-Preservation of Homogeneous Shear Flow Turbulence," Exp. Fluids, **13**, pp. 229–238.
[14] Comte-Bellot, G., and Corrsin, S., 1966, "The use of a Contraction to Improve the Isotropy of Grid-Generated Turbulence," J. Fluid Mech., **25**, pp. 657–682.
[15] Comte-Bellot, G., and Corrsin, S., 1971, "Simple Eulerian Time Correlation of Full- and Narrow-Band Velocity Signals in Grid-Generated, 'Isotropic' Turbulence," J. Fluid Mech., **48**, pp. 273–337.
[16] Warhaft, Z., and Lumley, J., 1978, "An Experimental Study of Temperature Fluctuations in Grid-Generated Turbulence," J. Fluid Mech., **88**, pp. 659–684.
[17] Rohr, J., Itsweire, E., Helland, K., and Van Atta, C., 1988, "An Investigation of the Growth of Turbulence in a Uniform Mean- Shear Flow," J. Fluid Mech., **187**, pp. 1–33.
[18] Gibson, M., and Kanellopoulos, V., 1988, "Turbulence Measurements in a Nearly Homogeneous Shear Flow," *Transport Phenomena in Turbulent Flows*, M. Hirat and N. Kasgi eds., pp. 17–28.
[19] George, W. K., and Castillo, L., 1997, "Zero-Pressure Gradient Turbulent Boundary Layer," Appl. Mech. Rev., **50**(12), pp. 689–729.
[20] Castillo, L., and George, W. K., 2001, "Similarity Analysis of Turbulent Boundary Layers with Pressure Gradient: Outer Flow," AIAA J., **39**(1), pp. 41–47.
[21] Cannon, S., Champagne, F., and Glezer, A., 1993, "Observations of Large-Scale Structure in Wakes Behind Axisymmetric Bodies," Exp. Fluids, **14**, pp. 447–450.
[22] Zhou, Y., and Antonia, R., 1994, "Effect of Initial Conditions on Characteristics of Turbulent Far Wake," JSME Int. J., Ser. B, **37**(4), pp. 718–725.
[23] Zhou, Y., and Antonia, R., 1995, "Memory Effects in a Turbulent Plane Wake," Exp. Fluids, **19**(2), pp. 112–120.
[24] Boersma, G., Brethouwer, G., and Nieuwstadt, F. T. M., 1998, "A Numerical Investigation of the Effect of the Inflow Conditions on the Self-Similar Region of a Round Jet," Phys. Fluids A, **10**(4), pp. 899–909.
[25] Rinoshika, A., and Zhou, Y., 2007, "Effects of Initial Conditions on Wavelet-Decomposed Structures in a Turbulent Far Wake," Int. J. Heat Fluid Flow, **28**, pp. 948–962.
[26] Moser, R. D., Rogers, M. M., and Ewing, D. W., 1998, "Self-Similarity of Time-Evolving Plane Wakes," J. Fluid Mech., **367**, pp. 255–289.
[27] Ewing, D., George, W., Rogers, M., and Moser, R., 2007, "Two-Point Similarity in Temporally Evolving Plane Wakes," J. Fluid Mech., **577**, pp. 287–307.
[28] Rogers, M. M., 2005, "Turbulent Plane Wakes Subjected to Successive Strains," J. Fluid Mech., **535**, pp. 215–243.
[29] Ghosal, S., and Rogers, M. M., 1997, "A Numerical Study of Self-Similarity in a Turbulent Plane Wake Using Large Eddy Simulation," Phys. Fluids A, **9**(6), pp. 1729–1739.
[30] Cannon, S., 1991, "Large-Scale Structures and the Spatial Evolution of Wakes Behind Axisymmetric Bluff Bodies," Ph.D. Thesis, University of Arizona, Tucson, AZ.
[31] Johansson, P. B. V., George, W. K., and Gourlay, M. J., 2003, "Equilibrium Similarity, Effects of Initial Conditions and Local Reynolds Number on the Axisymmetric Wake," Phys. Fluids A, **15**(3), pp. 603–617.
[32] Johansson, P. B. V., and George, W. K., 2006, "The Far Downstream Evolution of the High Reynolds Number Axisymmetric Wake Behind a Disk. Part 1. Single Point Statistics," J.Fluid Mech., **555**, pp. 363–385.
[33] Gourlay, M. J., Arendt, S., Fritts, D. C., and Werne, J., 2001, "Numerical Modeling of Initially Turbulent Wakes With Net Momentum," Phys. Fluids A, **13**, pp. 3783–3802.
[34] Panchepakesan, N. R., and Lumley, J., 1993, "Turbulence Measurements in Axisymmetric Jets of Air and Helium. Part 1. 34 Air Jet," J. Fluid Mech., **246**, p. 197–223.
[35] Hussein, H., Capp, S., and George, W. K., 1994, "Velocity Measurements in a High Reynolds Number, Momentum Conserving Axisymmetric Turbulent Jet," J. Fluid Mech., **258**, pp. 31–75.
[36] Cater, J., and Soria, J., 2002, "The Evolution of Round Zero-Net-Mass-Flux Jets," J. Fluid Mech., **472**, pp. 167–200.
[37] Parekh, D., Leonard, A., and Reynolds, W., 1988, "Bifurcating Jets at High Reynolds Numbers," Technical Report: Deptartment of Mechanical Engineering, Stanford University, Palo Alto, CA.
[38] Russ, S., and Strykowski, P., 1993, "Turbulent Structure and Entrainment in Heated Jets: The Effect of Initial Conditions," Phys. Fluids A, **12**(12), pp. 3216–3225.
[39] Grinstein, F., 2001, "Vortex Dynamics and Entrainment in Rectangular Free Jets," J. Fluid Mech., **437**, pp. 69–101.
[40] Grinstein, F. F., Glauser, M. M., and George, W. K., 2001, "Vorticity in Jets," *Fluid Vortices*, S. Greene, ed., Kluwer, Norwell, MA, pp. 65–88.
[41] Gilchrist, R., and Naughton, J., 2005, "Experimental Study of Incompressible Jets With Different Initial Swirl Distributions: Mean Results," AIAA J., **43**(4), pp. 741–751.
[42] Fukushima, C., Aanen, L., and Westerweel, J., 2000, "Investigation of the Mixing Process in an Axisymmetric Turbulent Jet using PIV and LIF," Proceedings of the 10th International Symposium on Applications of Laser Techniques to Fluid Mechanics, Lisbon, Portugal.
[43] Ewing, D., Frohnapfel, B., George, W., Pedersen, J., and Westerweel, J., 2007, "Two-Point Similarity in the Round Jet," J. Fluid Mech., **577**, pp. 309–330.
[44] Mi, J., Nobis, D. S., and Nathan, G. J., 2001, "Influence of Jet Exit Conditions on the Passive Scalar Field of an Axisymmetric Free Jet," J. Fluid Mech., **432**, pp. 91–125.
[45] Xu, G., and Antonia, R., 2002, "Effect of Different Initial Conditions on a Turbulent Round Free Jet," Exp. Fluids, **33**(5), pp. 677–683.
[46] Xu, G., and Antonia, R., 2002, "Effect of Initial Conditions on the Temperature Field of a Turbulent Round Free Jet," Int. Commun. Heat Mas Transfer, **29**(8), pp. 1057–1068.
[47] Burattini, P., and Djendidi, L., 2004, "Velocity and Passive Scalar Characteristics in a Round Jet With Grids at the Nozzle Exit," Flow, Turbul. Combust., **72**, pp. 199–218.
[48] Burattini, P., and Antonia, R., 2005, "Similarity in the Far Field of a Turbulent Round Jet," Phys. Fluids, **17**, p. 025101.
[49] Ferdman, E., Otugen, M. V., and Kim, S., 2000, "Effect of Initial Velocity Profile on the Development of Round Jets," J. Propul. Power, **16**, pp. 676–686.
[50] George, W., 1990, "Governing Equations, Experiments, and the Experimentalist," J. Exp. Therm. Fluid Sci., **3**, pp. 557–566.
[51] Shiri, A., George, W., and Naughton, J., 2006, "An Experimental Study of the Far-Field of Incompressible Swirling Jets," AIAA J., **46**(8), pp. 2002–2009.
[52] Morton, B., 1959, "Forced Plumes," J. Fluid Mech., **2**, pp. 151–163.
[53] Kotsovinos, N., and List, E., 1977, "Turbulent Buoyant Jet. Part 1. Integral Properties," J. Fluid Mech., **81**, pp. 25–44.
[54] Baker, C. B. T. D., and George, W., 1982, "An Analysis of Buoyant Jet Heat Transfer," Proceedings of the 7th International Heat Transfer Conference, Munich, Germany.
[55] Shabbir, A., and George, W., 1993, "Experiments on a Round Turbulent Buoyant Plume," J. Fluid Mech., **275**, pp. 1–32.
[56] Ewing, D., 1999, "Decay of Round Turbulent Jets With Swirl," *Proceedings of the 4th International Symposium on Engineering Turbulence Modeling and Experiments*, Elsvier, Amsterdam.
[57] Chigier, N., and Chervinsky, A., 1967, "Experimental Investigation of Swirling Vortex Motion in Jets," Trans. ASME J. Appl. Mech., **34**, pp. 443–451.
[58] Farokhi, S., Taghavi, R., and Rice, E., 1989, "Effect of Initial Swirl Distribution on the Evolution of a Turbulent Jet," AIAA J., **27**(6), pp. 700–706.
[59] Shiri, A. F., George, W. K., and Toutiaei, S., 2007, "Evaluation of Closure Hypotheses Using Recent Experimental Data on the Similarity Region of Swirling Jet Flows," Proceedings of 4th Ankara International Aerospace Conference, METU Turkey, Ankara, Sept. 10–12, Paper No. AIAC-2007-051.
[60] Shiri, A. F., Toutiaei, S., and George, W. K., 2007, "Turbulent Flow Structure in the Similarity Region of a Swirling Jet," *Proceedings of 11th EUROMECH European Turbulence Conference*, Porto, Portugal, Jun. 25–28, pp. 471–473.
[61] Bremhorst, K., and Hollis, P., 1990, "Velocity Field of an Axisymmetric Pulsed, Subsonic Air Jet," AIAA J., **28**, pp. 2043–2049.
[62] Batchelor, G. K., and Townsend, A. A., 1947, "Decay of Vorticity in Isotropic Turbulence," Proc. R. Soc. London Ser. A, **190**(1023), pp. 534–550.
[63] von Kármán, T., and Howarth, L., 1938, "On the Statistical Theory of Isotropic Turbulence," Proc. R. Soc. London Ser. A, **164**(917), pp. 192–215.
[64] Kistler, A., and Vrebalovich, T., 1966, "Grid Turbulence at Large Reynolds Number," J. Fluid Mech., **26**, pp. 37–47.
[65] Reynolds, W., 1976, "Computation of Turbulent Flows," Ann. Rev. Fluid Mech., **8**, pp. 183–208.
[66] Batchelor, G., 1953, *Homogeneous Turbulence*, Cambridge University Press, Cambridge, UK.
[67] Monin, Y., and Yaglom, Y., 1972, *Statistical Fluid Mechanics, Vol II*, MIT Press, Cambridge, MA.
[68] Yeung, P., Brasseur, J., and Wang, Q., 1995, "Dynamics of Direct Large-Small Scale Couplings in Coherently Forced Turbulence: Concurrent Physical- and Fourier-Space Views," J. Fluid Mech., **283**(4), pp. 43–95.
[69] Citriniti, J. H., and George, W. K., 1997, "The Reduction of Spatial Aliasing by Long Hot-Wire Anemometer Probes," Exp. Fluids, **23**, pp. 217–224.
[70] Wang, H., and George, W. K., 2002, "The Integral Scale in Homogeneous Isotropic Turbulence," J. Fluid Mech., **459**, pp. 429–443.
[71] Batchelor, G., 1948, "Energy Decay and Self-Preserving Correlation Functions in Isotropic Turbulence," Q. Appl. Math., **6**, pp. 97–116.
[72] Batchelor, G., and Townsend, A., 1948, "Decay of Isotropic Turbulence in the Initial Period," Proc. R. Soc. London Ser. A, **193**, pp. 539–558.
[73] Mills, R., Kistler, A., O'Brien, V., and Corrsin, S., 1958, "Turbulence and Temperature Fluctuations behind a Heated Grid," Johns Hopkins University, NACA Tech. Note No. 4288.
[74] Frenkiel, F. N., and Klebanoff, P., 1971, "Statistical Properties of Velocity Derivatives in a Turbulent Field," J. Fluid Mech., **48**, pp. 183–208.
[75] Bennett, J., and Corrsin, S., 1978, "Small Reynolds Number Nearly Isotropic Turbulence in a Straight Duct and Contraction," Phys. Fluids, **21**, pp. 2129–2141.
[76] Kolmogorov, A., 1963, "A Refinement of Previous Hypothesis Concerning the Local Structure of Turbulence in a Viscous Incompressible Fluid at High Reynolds Number," J. Fluid Mech., **13**, pp. 82–85.
[77] Kolmogorov, A., 1941, "The Local Structure of Turbulence in Incompressible Viscous Fluid for Very Large Reynolds Numbers," C. R. Akad. Sci. SSSR, **30**, p. 301.
[78] Tavoularis, S., and Karnik, U., 1989, "Further Experiments on the Evolution of Turbulent Stresses and Scales in Uniformly Sheared Turbulence," J. Fluid Mech., **204**, pp. 457–478.

[79] Tavoularis, S., 1985, "Asymptotic Laws for Transversely Homogeneous Turbulent Shear Flows," *Phys. Fluids*, **28**, pp. 999–1001.
[80] Tavoularis, S., and Corrsin, S., 1981, "Experiments in Nearly Homogenous Turbulent Shear Flow With a Uniform Mean Temperature Gradient. Part 1," J. Fluid Mech., **104**, pp. 311–347.
[81] Harris, V., Grahm, J., and Corrsin, S., 1977, "Further Experiments in Nearly Homogeneous Shear Flow". J. Fluid Mech., **81**, pp. 657–687.
[82] Wray, A., 1998, "Decaying Isotropic Turbulence," AGARD Advis. Rep., **345**, pp. 63–64.
[83] de Bruyn Kops, S., and Riley, J., 1999, "Direct Numerical Simulation of Laboratory Experiments in Isotropic Turbulence," Phys. Fluids A, **10**, pp. 2125–2127.
[84] Wang, H., Gamard, S., Sonnenmeier, J. R., and George, W. K., 2000, "Evaluating DNS of Isotropic Turbulence using Similarity Theory," Proceedings of the ICTAM 2000, Chicago, IL, 27 Aug.–1 Sept. 2000.
[85] George, W., Wang, H., Wollblad, C., and Johansson, T., 2001, "Homogeneous Turbulence and its Relation to Realizable Flows," *Proceedings of the 14th Australasian Fluid Mechanics Conference*, Adelaide, S. Australia, Dec. 2001, pp. 41–48.
[86] Antonia, R., Smalley, R., Zhou, T., Anselmet, F., and Danaila, L., 2003, "Similarity of Energy Structure Functions in Decaying Homogeneous Isotropic Turbulence," J. Fluid Mech., **487**, pp. 245–269.
[87] Antonia, R., and Orlandi, P., 2004, "Similarity of Decaying Isotropic Turbulence With a Passive Scalar," J. Fluid Mech., **505**, pp. 123–151.
[88] Lavoie, P., Burattini, P., Djendidi, L., and Antonia, R., 2005, "Effect of Initial Conditions on Decaying Grid Turbulence at Low $R\lambda$," Exp. Fluids, **39**, pp. 865–874.
[89] Burattini, P., Lavoie, P., Agrawal, A., Djendidi, L., and Antonia, R., 2006, "Power Law of Decaying Homogeneous Isotropic Turbulence at Low Reynolds Number," Phys. Rev. E, **73**, p. 066304.
[90] Hurst, D., and Vasillicos, J., 2007, "Scalings and Decay of Fractal-Generated Turbulence," Phys. Fluids, **19**, p. 035103.
[91] Lavoie, P., Djendidi, L., and Antonia, R., 2007, "Effects of Initial Conditions in Decaying Turbulence Generated by Passive Grids," J. Fluid Mech., **585**, pp. 395–420.
[92] George, W. K., and Wang, H., 2002, "The Spectral Transfer in Isotropic Turbulence," *Proceedings of the IUTAM Symposium On Reynolds Number Scaling in Turbulent Flow*, Princeton, NJ, Sept. 11–13, Kluwer, MA.
[93] Kang, H., Chester, S., and Meneveau, C., 2003, "Decaying Turbulence in an Active-Grid-Generated Flow and Comparisons With Large-Eddy Simulation," J. Fluid Mech., **480**, pp. 129–160.
[94] Hurst, D., 2006, "Wind Tunnel Experiments in Fractal Induced Turbulence," Ph. D. Thesis, Deptartmemt of Aeronautics, Imperial College of London, London, UK.
[95] Seoud, R., and Vassilicos, J., 2007, "Dissipation and Decay of Fractal-Generated Turbulence," Phys. Fluids, **19**, p. 105108.
[96] George, W. K., and Wang, H., 2009, "The Exponential Decay of Homogenous Turbulence," Phys. Fluids, **21**, p. 025108.
[97] Krogstad, P., and Davidson, P., 2011, "Freely Decaying Homogeneous Turbulence Generated by Multi-Scale Grids," J. Fluid Mech., **680**, pp. 417–434.
[98] Valente, P., and Vassilicos, J., 2011, "Dependence of Decaying Homogeneous Isotropic Turbulence on Inflow Conditions," Phys. Lett. A, **376**, pp. 510–514.
[99] Loitsianskii, L., 1939, "Some Basic Laws for Isotropic Turbulence," Tech. Report 440, Central Aero- Hydrodynamic Institute, Moscow, (translated as NACA Tech. Memo 1079).
[100] Vassilicos, J., 2011, "An Infinity of Possible Invariants for Decaying Homogeneous Turbulence," Phys. Lett. A, **375**, p. 1010–1019.
[101] Gustafsson, J., and George, W., 2011, "Energy Spectra at Low Wavenumbers in Homogeneous Incompressible Turbulence," Phys. Lett. A, **375**, pp. 2850–2853.
[102] Nelkin, M., 1996, "Universality and Scaling in Fully Developed Turbulence," Adv. Phys., **43**, pp. 143–181.
[103] George, W., and Tutkun, M., 2009, "Mind the Gap: A Guideline for Large Eddy Simulation," Philos. Trans. R. Soc. A, **367**, pp. 2839–2847.
[104] Champagne, F., 1978, "The Fine-Scale Structure of the Turbulent Velocity Field," J. Fluid Mech., **86**, pp. 67–108.
[105] Tennekes, H., and Wyngaard, J., 1972, "The Intermittent Small-Scale Structure of Turbulence: Data-Processing Hazards," J. Fluid Mech., **55**, pp. 93–103.
[106] Lumley, J., 1965, "Interpretation of Time Spectra in High Intensity Shear Flow," Phys. Fluids, **8**, pp. 1056–1063.
[107] Burattini, P., Lavoie, P., and Antonia, R., 2008, "Velocity Derivative Skewness in Isotropic Turbulence and its Measurement with Hot Wires," Exp. Fluids, **45**, pp. 523–535.
[108] Mazellier, N., and Vassilicos, J., 2010, "Turbulence Without Richardson-Kolmogorov Cascade," Phys. Fluids, **22**, p. 075101.
[109] Gamard, S., and George, W., 2000, "Reynolds Number Dependence of Energy Spectra in the Overlap Region of Isotropic Turbulence," J. Flow Turbul. Combust., **63**, pp. 443–477.
[110] Slessor, M. D., Bond, C. L., and Dimotakis, P. E., 1998, "Turbulent Shear-Layer Mixing at High Reynolds Numbers: Effects of Inflow Conditions," J. Fluid Mech., **376**, pp. 115–138.
[111] Ristorcelli, J. R., and Clark, T. T., 2004, "Rayleigh-Taylor Turbulence: Self-Similar Analysis and Direct Numerical Simulations," J. Fluid Mech., **507**, pp. 213–253.
[112] Ramaprabhu, P., Dimonte, G., and Andrews, M., 2005, "A Numerical Study of the Influence of Initial Perturbation on the Turbulent Rayleigh-Taylor Instability," J. Fluid Mech., **536**, pp. 285–319.
[113] Mueschke, N., Andrews, M., and Schilling, O., 2006, "Experimental Characterization of Initial Conditions and Spatio-Temporal Evolution of a Small-Atwood-Number Rayleigh-Taylor Mixing Layer," J. Fluid Mech., **567**, pp. 27–63.
[114] Youngs, D., 2008,"Turbulent Mixing due to Rayleigh-Taylor Instability," Bull. Am. Phys. Soc., **53**(15), p. 123102.
[115] Arndt, R., and Wosnik, M., 2006, "Experimental and Numerical Investigation of Large Scale Structures in Cavitating Wakes," *Proceedings of the 36th AIAA Fluid Dynamics Conference and Exhibit*, AIAA Paper No. 2006–3046.
[116] Cal, R., Brzek, B., Johansson, T., and Castillo, L., 2006, "Upstream Condition Effects on Rough Favorable Pressure Gradient Turbulent Boundary Layers," *Proceedings of the 44th AIAA Aerospace Sciences Meeting and Exhibit*, Reno, NV, Jan. 9–12, AIAA Paper No. AIAA-2006-3271.
[117] Druault, P., Lardeau, S., Bonnet, J.-P., Coiffet, F., Delville, J., Lamballais, J. F. L. J., and Perret, L., 2004, "A Methodology for the Generation of Realistic 3-D Turbulent Unsteady Inlet Conditions for Les Computations," AIAA J., **42**(3), pp. 447–456.